e-Newsletter n°3

June 2008
Available at http://www.ist-brighter.eu

WWW.BRIGHTER.EU

World Wide Welfare: High-Brightness Semiconductor Lasers for Generic Use

WWW.BRIGHTER.EU is an integrated project supported by the European Commission's Information Society Technologies programme

CONTENT

EDITORIAL

Welcome to the 3rd e-Newsletter of the 3 year integrated project WWW.BRIGHTER.EU, which began in October 2006. This integrated project builds upon the earlier WWW.BRIGHT.EU project, in which we published our first series of e-Newsletters.

If you missed either of the previous two editions of our e-Newsletter, then please visit our website to download your copy. The next e-Newsletter will be published in October 2008.

We hope you will enjoy reading this e-Newsletter and learning about the latest developments in our project.

The Editors

Steve Bull
University of Nottingham
steve.bull@nottingham.ac.uk

Myriam Oudart
Alcatel Thales III-V lab
myriam.oudart@3-5lab.fr

Eric Larkins
University of Nottingham
eric.larkins@nottingham.ac.uk

GREETINGS FROM THE PROJECT COORDINATOR

Michel Krakowski
Project Coordinator
Alcatel Thales III-V Lab
michel.krakowski@3-5lab.fr

Dear Reader,

Welcome to the third e-Newsletter of our EC-IST Project ***World Wide Welfare: High-Brightness Semiconductor Lasers for Generic Use (WWW.BRIGHTER.EU)***, an Integrated Project on high-brightness laser diode technologies and applications, which began in October 2006.

Since our last e-Newsletter, we've again been working hard towards the project objectives and continue to be successful across a wide range of project areas – both technological / scientific and in the training of young researchers and project outreach activities. You may have seen our recent press release reporting on the BRIGHTER project, which has been widely distributed in the scientific media. If you missed this and would like a copy, please just let us know. You may also have met members of our Consortium and seen some of our newest results and partner exhibits at large events such as Photonics West and CLEO. We have now produced a short video introduction to the BRIGHTER project and this was shown at the beginning of a recent workshop. It will be available via our website in the next few weeks. Indeed, over the coming weeks, we will be updating our website *www.ist-brighter.eu* with new information about the project and many new materials to download and I encourage you to visit.

Inside this e-Newsletter you will find an update on some of the latest technical achievements within the project followed by profiles of four more project partners. There are also four extended articles in this e-Newsletter. Two applications topics cover the use of Raman fibre lasers in WDM transmission systems and also the use of high brightness diode laser sources for display applications. Technical papers are presented on overgrowth-free high power single mode lasers and on the development and application of a spectral laser model. There are also further items including a report on a project workshop on Toxicology and Safety in III-V Epitaxy and an introduction to our RichMedia CD format, which we are using to distribute tutorial and workshop presentations to the wider scientific and educational community. At the end of this edition, you can find details of some of our recent publications, a calendar of forthcoming events and a preview of the next e-Newsletter.

Michel Krakowski

TECHNICAL ACHIEVEMENTS

Towards the Project Objectives

The WWW.BRIHGTER.EU Project Consortium continues to be successful across the broad range of areas in the project. Here, we present a short review of some recent highlights ranging from high wallplug efficiency near infrared laser bars and a high power blue source achieved through frequency-doubling to the investigation of catastrophic optical damage in red lasers and experimental and simulation results for a Raman fibre laser.

Understanding the catastrophic optical damage (COD) process in high-power red-emitting laser diodes

The dynamics of the COD process have been analysed for high-power red-emitting AlGaInP BA lasers under cw operation using thermal and optical near-field imaging. A clear temperature spike is observed after only 2.3ms at the location where the COD is seeded and this is followed by a jump in the entire device temperature. This study strongly suggests that the COD process of these lasers is due to a thermal runaway process.

M. Ziegler et al., Applied Physics Letters, Vol. 92, 103514, Mar. 2008.

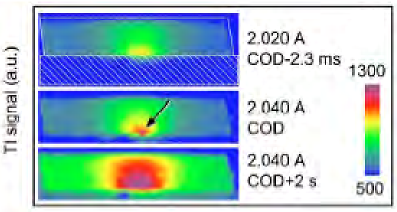

Raw thermal images of front facet before, at, and 2s after COD at the location marked.

New high-power blue laser source based on SHG in PPKTP

A 404nm laser system based on second harmonic generation in a compact external cavity configuration has been realised. The pump is an external cavity grating feedback 808nm tapered laser with a PPKTP crystal used for the SHG. A stable cw diffraction limited output of 318mW is obtained with a mode-matched pump power of 630mW. Up to 620mW of SHG power is obtained when the cavity is operated in a scanning mode.

J. Holm et al., Optics Express, Vol. 16, pp. 2486-2493, Feb. 2008.

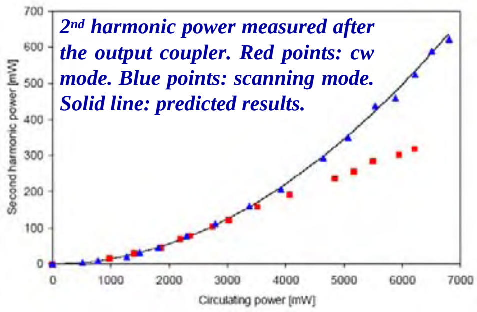

2nd harmonic power measured after the output coupler. Red points: cw mode. Blue points: scanning mode. Solid line: predicted results.

High power, high wallplug efficiency 975nm BA laser bars

Based on an Al-free active region with a strain compensated quantum well, a high wall-plug efficiency (WPE) of 68% has been obtained from a 975nm broad-area laser bar. For the 1cm laser bar containing 24 emitters, each of which is 120µm wide and has a cavity length of 2mm, a high power of 72W with a WPE of 67% has been achieved at 70A. On the same bar, the WPE reaches a maximum of 68% at 50W.

N. Michel et al., to be presented at the International Semiconductor Laser Conference (ISLC), Sorrento, Italy, 14th – 18th Sept. 2008.

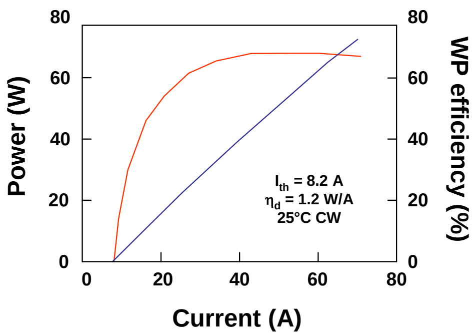

Raman fibre laser – Experiment and simulation

Simulated and experimental results of a two-output wavelength (1427nm and 1480nm) Raman fibre laser made of embedded cavities, and pumped by a 1117nm Yb fibre laser, have been compared. The thresholds and slopes of the simulated laser agree with the experiments, with a discrepancy of <10%. This error is in line with the measurement uncertainties of the system components.

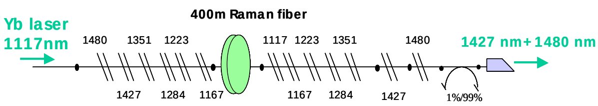

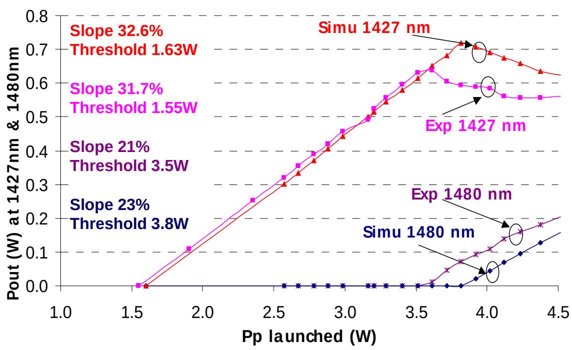

Results obtained by Alcatel-Lucent Bell Labs, 2008

PARTNER PRESENTATIONS

In this section of the e-Newsletter, we introduce some of the partners in the project Consortium. In this edition, profiles are presented for Keopsys S.A., OSRAM Opto-semiconductor GmbH, the Max Born Institute and the University of Würzburg.

KEOPSYS

Keopsys is headquartered in Lannion France, with an advanced R&D laboratory in Fairfax, Virginia and a sales office in Bethlehem, Pennsylvania.

Initially founded in 1997 by Marc Le Flohic, under the name of OptoCom Innovation, the company underwent significant expansion and was re-founded under the new name of Keopsys.

Keopsys has attracted a team with a demonstrated record of technical expertise and innovation, with approximately 40% of its workforce holding advanced degrees. The company maintains successful technical collaborations with research laboratories, universities and companies around the world.

1. FIBRALITE, OEM Raman Fibre Laser
2. SPIDERLITE, Multiple Ports High-Power Fibre Amplifier
3. MIRVISION, Eye-Safe High-Power Laser Transmitter
4. KULT, Eye-Safe Ultra-Compact Laser Transmitter
5. BENCHTOP, 1µm or 1.5µm Fibre Amplifiers and Lasers

Keopsys manufactures a large range of standard and custom-designed optical fibre amplifiers and lasers for fibre and free space optical communication systems, fibre-to-the-home (FTTH), component testing, remote sensing, spectroscopy, materials processing, medical, range-finding, 3D-scanning, military and research applications. High output powers are achieved through the use of double cladding fibres pumped by broad stripe diodes. A variety of pumping techniques are utilised, each optimised for a specific application.

In addition to conventional multimode fibre couplers, many Keopsys products also use a proprietary V-groove side-pumping (VSP®) technique to efficiently inject the pump light directly into double cladding fibres.

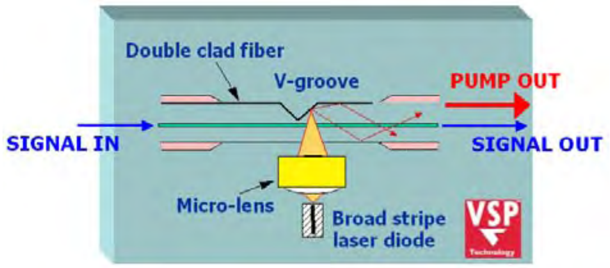

V-groove side-pumping technique (VSP®)

This approach offers higher conversion efficiency, smaller size, simpler assembly and shorter signal paths than are possible with other pumping methods.

Activities within WWW.BRIGHTER.EU

The role of Keopsys in BRIGHTER is to bring its experience in the manufacturing of high power fibre amplifiers and lasers to the Consortium.

The objective in the BRIGTHER project is to design and manufacture two prototypes: a Raman Fibre Laser and a Cladding-Pumped Erbium Doped Fibre Amplifier. The two designs are based on high-brightness and high-power pumps developed by other partners of the Consortium.

The two prototypes will be then used by Alcatel-Lucent for experiments in telecom applications.

Further Information

Further information can be obtained from:
KEOPSYS S.A.
Tel: +33 2 96 05 08 00
Fax: +33 2 96 05 08 01
Email: websales@keopsys.com
Web: http://www.keopsys.com

OSRAM Opto Semiconductors

Innovation driver for the future of light

Winning the 2007 German Future Prize has placed the researchers at OSRAM Opto Semi-conductors in the ranks of exceptional German scientists and developers, including some Nobel prize winners. The award for outstanding technical innovations, presented by the German President, was the latest highlight in the research history of OSRAM Opto Semiconductors, which stretches back more than thirty years. The company has long been one of the most innovative outfits in Germany. As one of the world's leading manufacturers of optoelectronic semiconductors for the lighting, sensor and visualization sectors, OSRAM Opto Semiconductors regularly launches new technologies and products that make a lasting difference to these sectors.

More than three decades of experience in the development and manufacture of optoelectronic semiconductor components have made OSRAM Opto Semiconductors one of the most significant innovation and technology drivers in Germany. Impressive evidence of this is provided by more than 3000 patents in various areas of semiconductor technology. Added to this is the wealth of experience in the lighting sector stretching back 100 years that the parent company OSRAM contributes.

The company focuses on innovative light sources in growing markets such as external automotive lighting, LED backlighting for LCD displays, projection applications, sensors for mobile applications and organic as well as standard light emitting diodes.

In the **automotive sector,** OSRAM Opto Semiconductors is the world market leader with its pioneering lighting solutions. The company's LEDs can be found in large numbers in dashboards, reading lights and other interior lights. LEDs have also started their triumphant march into exterior automotive lighting. Beside rear light clusters, the development of white emitting LEDs has advanced so far that these light sources will be used in headlights for the first time this year.

OSRAM Opto Semiconductors is taking a dual approach to **display and projection technology** with its LEDs and lasers. Small and medium-size screens (e.g. for sat-nav systems, LCD monitors, mobile phones and other mobile terminals) are already available with LED and OLED backlighting. For projection applications the company is using laser technology in addition to LED systems.

Rapid progress in the development of powerful high-brightness LEDs is opening up new opportunities for using these lighting solutions in entirely new markets. In the **general lighting** sector, LEDs are rapidly taking over from incandescent lamps. As point light sources, light emitting diodes are being used in more and more different applications. The range of use is rounded off by all types of signalling equipment such as traffic lights and railway signals. OLEDs will also be increasingly used in a variety of interesting applications in general lighting.

Our vast experience with **semiconductor lasers** is applied to devices addressing material processing, pumping solid state lasers, medical applications and sensing. For example, a major contribution to road safety is the Night Vision System that OSRAM Opto Semiconductors is developing in conjunction with a series of partners. Infrared light from our high-power lasers is used in addition to conventional headlights.

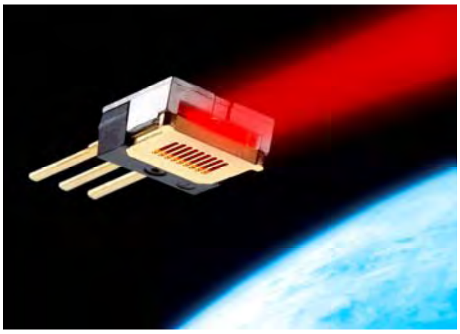

Red-emitting laser bar.

Activities within WWW.BRIGHTER.EU

Within BRIGHTER, OSRAM Opto Semiconductors develops multi-Watt 635 nm laser bars for photodynamic therapy (PDT). This activity comprises the epitaxial growth of laser structures, the fabrication of laser bars and finally the mounting into a package as shown above. Comprehensive characterisation is performed together with the Max-Born-Institute and the University of Nottingham. Biolitec integrates our red laser modules into systems ready to be deployed in the field. Regarding display applications OSRAM communicates the specs for high-brightness green and red lasers based on related marketing information. Comprehensive testing of high-brightness laser sources for noise, stability, modulation, brightness, power and integration into simple projection displays will be performed. OSRAM is already present in the target markets and is therefore well positioned to commercialise results. Besides contributing to achieving the technical objectives, OSRAM will identify major routes for exploiting (frequency-doubled) tapered lasers by developing applications and establishing connections to the end-users.

Further Information

Further information can be obtained from:

Dr. Martin Reufer
E-mail: martin.reufer@osram-os.com
Web: http://www.osram-os.com

Max-Born-Institute

The Max Born Institute (MBI) for Nonlinear Optics and Short Pulse Spectroscopy was founded in 1992. It belongs to the "Forschungsverbund Berlin e.V." and is a member of the "Leibniz Association". The MBI has about 180 members of staff of which 90 are scientists (including PhD students).

The MBI conducts basic research in the field of nonlinear optics and ultra fast dynamics of the interaction of light with matter and furthermore pursues applications which emerge from this research. For these investigations, laser-based short-pulse light sources in a broad spectral range from the mid-infrared, through the visible, down to the x-ray wavelength region are used.

The Max Born Institute within Berlin Adlershof – the City of Science, Technology and Media.

With its research the MBI fulfils a nationwide mission and is an integral part of the international science community. It offers its facilities and scientific know-how to external researchers through an active guest programme. The MBI is involved in a large number and variety of cooperative research projects with universities, research institutions and industrial partners.

The group "Optoelectronic Devices" at the MBI performs research on the application of spectroscopic techniques developed or improved upon at the MBI to analytical purposes in optoelectronic devices. A primary objective is to improve insight into the microscopic nature of the mechanisms defining the limits of semiconductor device operation. The following themes are the present focus of the groups' research activities:

- Defect creation and accumulation within the active region of semiconductor devices
- Mechanical stress
- Device and facet heating mechanisms including the catastrophic optical damage effect

All of the above are quantitatively analysed in a wide range of very different device structures.

Together with our industrial partners new generations of optoelectronic devices with increased brightness and reliability are created, taking into account the analytical results from the MBI. Investigations of transient recombination processes (sub ps - ns) in optoelectronic materials such as quantum-well or quantum-dot structures complete these device-related analytical activities. Carrier transfer kinetics in self-assembled or structured nanostructures are also addressed.

Activities within WWW.BRIGHTER.EU

Within the BRIGHTER project, MBI coordinates Workpackage 5 – Reliability. In this Workpackage, MBI provides and applies analytical tools that help our understanding of the gradual degradation processes in high-power, high-brightness laser diodes. This involves the application of non-destructive analytical optical techniques such as photocurrent spectroscopy, laser beam induced current, electroluminescence, thermal imaging, Raman-spectroscopy and steady-state and transient photoluminescence spectroscopy. Within joint experiments, such as "by-emitter" analysis of laser arrays, these activities help to fulfil the objectives of Workpackage 5.

Students & staff of the "Optoelectronic Devices" group.

Further Information

Further information can be obtained from:
Dr. Jens W. Tomm
Tel: + 49 (0)30 6392 1453
Fax: + 49 (0)30 6392 1459
Email: tomm@mbi-berlin.de
Web: http://www.mbi-berlin.de

University of Würzburg

The group of the university which is involved in the BRIGHTER project is part of the chair for 'Technische Physik', which was established in 1990 at the physics department of the university. The research activities are focussed on studying basic physical properties of low dimensional photonic and electronic semiconductors and on the development of novel optoelectronic devices. A complete process chain for III-V semiconductors is available in the micro-fabrication laboratory (550 m^2 clean room) of the group. Solid and gas source molecular beam epitaxy (MBE) systems for different III-V material systems (GaIn(N)As/AlGaAs, InGaAsP/InP and InGaSbAs/GaSb) provide the layer structures for the subsequent processing. A combination of optical, e-beam, ion-beam and imprint lithography together with different dry etching and deposition systems are used for the lateral patterning. The clean room also houses some process-related characterisation, such as electron microscopy and a secondary ion mass spectrometer.

In addition to the fabrication capabilities, the group operates a number of laboratories for the investigation of nano-scale semiconductors by optical spectroscopy and transport experiments. Several setups are available for device characterisation, including facilities for pulsed and continuous wave measurements of lasers and measurements of various dynamic properties such as modulation bandwidth, noise, linewidth and chirp.

The device related research of the group is typically carried out in close collaboration with partners from large companies (e.g. III-V lab, Alcatel, Thales R&T and OSRAM) and SMEs in the frame of European or national projects. The research group has been or is still active as coordinator or partner in a range of different European projects (e.g. NANOPT, NANOLASE, QSWITCH, WWW.BRIGHTER.EU, ULTRABRIGHT, NANO-TCAD, BIGBAND, FUNFOX).

Electron-beam lithography system.

A major objective of the optoelectronics related research during the past few years has been the development of novel laser structures for high power, sensing and telecommunication applications. Examples are InGaAs/AlGaAs quantum dot lasers grown by MBE with record high output powers at 980 nm. For the realisation of long wavelength lasers on GaAs substrates, devices with active regions based on InAs quantum dots or GaInNAs quantum wells have been investigated. The longest wavelength achieved with an GaInNAs active region was 1.5 µm. Quantum dash structures on InP are used in the wavelength range between 1.45 µm and 1.8 µm. Even longer wavelengths are available by the use of GaSb based lasers or by the use of quantum cascade structures. Complex-coupled distributed feedback lasers based on lateral feedback gratings have been realised on all the material systems listed above. This technique has also been used to fabricate single-mode widely tuneable lasers. The group is also active in developing photonic crystal based opto-electronic devices. An example is tuneable laser sources with an on-chip wavelength monitor that have been realised by integration of photonic crystal waveguides, mirrors and filters with a semiconductor laser.

Activities within WWW.BRIGHTER.EU

Within the BRIGHTER project, the group is mainly contributing to the development of single-mode tapered laser diodes. The goal is to introduce frequency selective elements (gratings) in the cavity of a tapered laser in order to restrict the emission of the devices to a narrow spectral region or even a single wavelength. This is required, for example, when the output of the laser is frequency doubled or in pumping a gain media with narrow absorption lines. In addition to the spectral narrowing, the gratings reduce the shift of the emission wavelength with temperature by a factor of three compared to standard tapered lasers. The focus is on the development of overgrowth-free fabrication techniques, where the laser layer is grown in a single epitaxy step and the grating is added afterwards. This approach is advantageous in terms of process complexity, yield and reliability. Both lateral gratings in the ridge waveguide section and distributed Bragg reflectors at the end of the ridge waveguide have been successfully used to realise single-mode tapered lasers.

Further Information

Further information can be obtained from:

Dr. Martin Kamp
Tel: +49 931 888 5121
E-mail: martin.kamp@physik.uni-wuerzburg.de
Web: http://tep.physik.uni-wuerzburg.de

Multi-Wavelength Power-Adjustable Raman Fibre Laser for Broadband Dynamic Gain Amplification

Marc Le Flohic, Christophe Vitre, Sylvain Bordais

Keopsys S.A., 21 rue Louis de Broglie, 22300 Lannion, FRANCE

Tel: +33 2 96 05 08 00 Fax: +33 2 96 05 08 01 Email: cvitre@keopsys.com

Abstract: Wavelength-Division-Multiplexed (WDM) transmission systems based on Erbium-Doped Fibre Amplifiers (EDFAs) with aggregate capacities of more than 1 Tb/s have been demonstrated using the entire band of EDFAs, i.e. both the C- and L-bands. The transmission performance is mainly determined by the Optical Signal-to-Noise Ratio (OSNR) and the waveform distortion due to the non-linear effects. Raman amplification offers several advantages to increase capacities: bit rate independence, noise figure improvement, wide bandwidth, compatibility with existing systems.

The advantage of Raman amplification is that it can be obtained at "any wavelength", even where the use of rare ion doped fibre is not possible. Moreover, Raman amplification is distributed along the transmission fibre which is used as an amplification medium resulting in a reduced degradation of the OSNR. The system input power to achieve the required OSNR can be reduced in order to avoid signal distortions due to non-linear effects. In the first section, the fundamentals of Raman amplification are presented. The second section focuses on WDM system architectures in which Distributed Raman Amplification (DRA) is employed. Large Raman gain bandwidth can be achieved using multiplexed pump laser diodes. An alternative solution consists of the multi-wavelength Raman Fibre Laser. The performance of a high-power 3-wavelength Raman Fibre Laser (3λ-RFL) over well selected wavelengths (1428 nm, 1445 nm, 1466 nm) is presented. The interdependence of the optical power at different wavelengths in the single cavity has a relatively low sensitivity. Thus, the Raman gain profile can be dynamically adjusted over the C-band independent of the fibre type used. Also, the 3λ-RFL architecture does not significantly increase the complexity of the Cascade Raman Laser resonator architecture. Therefore, the multi-wavelength-RFL is a promising solution for broadband Raman amplification.

Introduction

The principle of Raman amplification is based on the stimulated emission process associated with Raman scattering. The first observation of Raman amplification in an optical fibre was obtained by Stolen and Ippen [1] in 1973. When an optical signal (referred to as the Pump) propagates in an optical fibre, it experiences scattering caused by molecular vibrations (optical phonons). The scattered light is frequency-shifted by an amount equal to the difference between the pump frequency and the molecular vibrational frequency of the glass as presented in Fig. 1. This shifted signal is referred to as the Stokes field and the non-linear optical effect that gives rise to it is known as Raman scattering. When the Stokes signal mixes again with the original pump, this gives rise to a resonant interaction and the Stokes signal is amplified. This corresponds to the Stimulated Raman Scattering (SRS) effect. The amorphous structure of the glass produces broadband vibrational frequencies which depend on the fibre properties. Thus, the Raman Stokes shift also exhibits a broad continuum shape. The Stokes shift has a maximum at 13.2 THz for germano-silicate fibre as shown in Fig. 2. For a pump at 1445 nm, the maximum Stokes signal is at 1537 nm. The corresponding useful 3 dB bandwidth of gain extends over 30 nm. When a signal is seeded around this wavelength, it experiences stimulated amplification via Raman amplification.

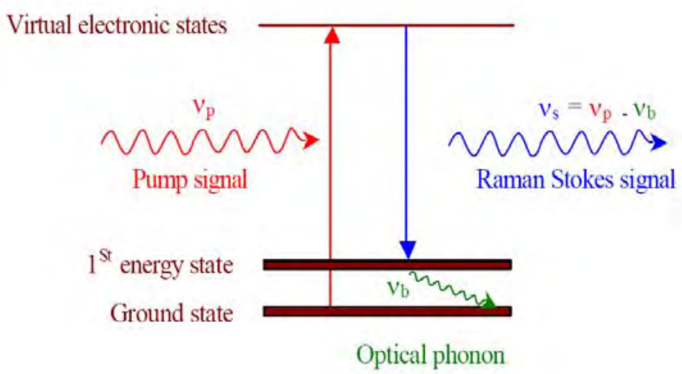

Fig. 1: Energy levels and transitions involved in the SRS process.

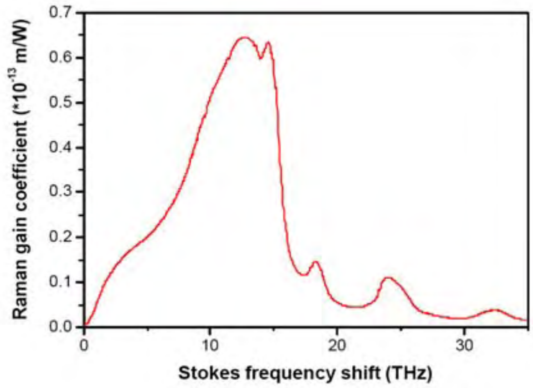

Fig. 2: Raman gain spectrum of a pure silica fibre.

Figure 3 illustrates a general scheme of a Raman amplifier. The gain of a Raman amplifier can be expressed as:

$$G_{On-Off} = \exp\left(g_R \frac{P_{pump}}{A_{eff}} L_{eff} \right)$$

where g_R is the Raman gain coefficient, P_{pump} the pump power injected into the fibre, A_{eff} the effective fibre core area and L_{eff} is the non-linear effective length. $G_{On\text{-}Off}$ is referred to as the On/Off gain, because it characterises the output signal power when the pump is turned on relative to the power when the pump is turned off (the signal is then attenuated by the fibre).

This relation shows that Raman amplification acts as soon as pump power exists (i.e. there is no pump threshold). If we use typical parameters of g_R = 10-13 m/W, L_{eff} = 10 km, A_{eff} = 80 µm^2, then a 20 dB Raman gain is obtained for P_{pump} ~ 350 mW. There is also a polarisation Raman gain dependence through the g_R parameter. If the pump and the signal are polarised, the resulting g_R is equal to g_R x 0% in the case of perpendicular polarisations and g_R x 100% in the case of parallel polarisations. If the pump is non-polarised and the signal is polarised, the resulting average g_R is g_R x 50%.

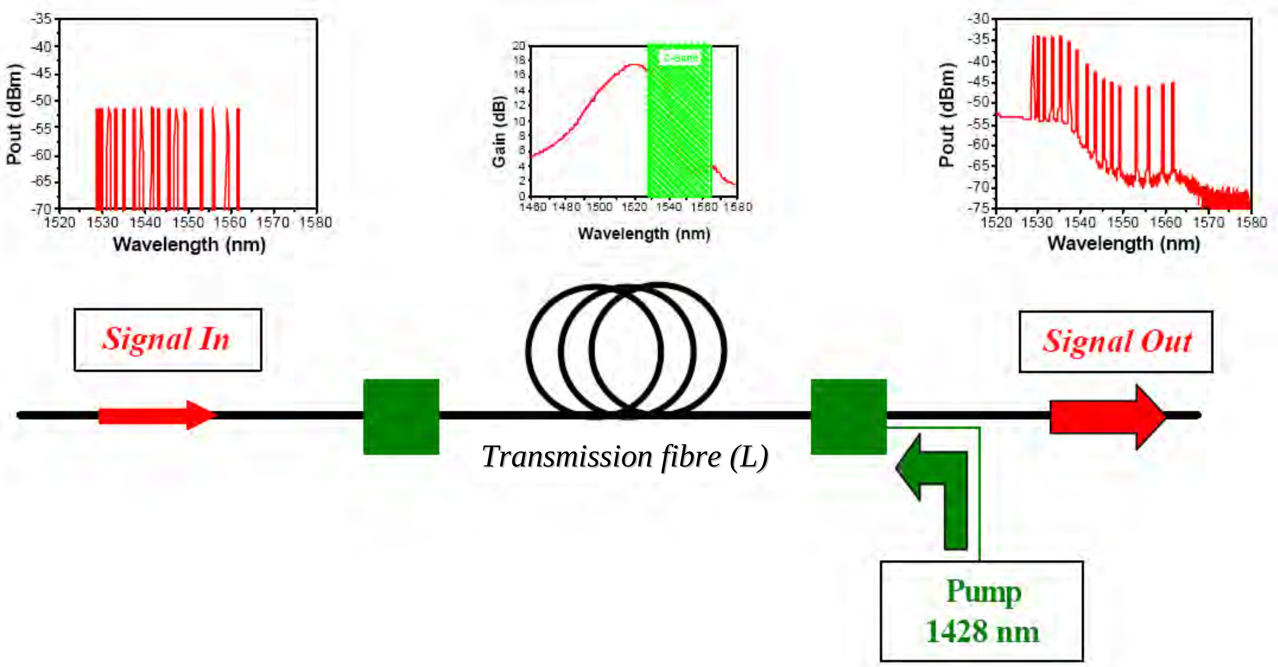

Fig. 3: General scheme of a Raman amplifier in a backward pumping configuration.

Distributed Raman Amplification (DRA) allows one to achieve less fibre loss by utilising the transmission fibre as an amplification medium. DRA can be represented as a chain of closely spaced amplifiers with small lumped gain. The ASE noise generated in one of these discrete amplifiers distributed along the transmission fibre span is reduced when arriving at the receiver input. Therefore, the noise power P_{ASE} at the receiver is reduced by using DRA when compared with the case of the same lumped EDFA located at the end of the transmission fibre span. This P_{ASE} reduction induces a significantly lower OSNR degradation. This OSNR improvement can be expressed in terms of Equivalent Noise Figure (NF_{eq}) using the relationship:

$$NF_{eq} = \frac{1}{G_{On-Off}} + \frac{P_{ASE}}{G_{On-Off}\, h\nu B_o}$$

where $G_{On\text{-}Off}$ is the On-Off gain, P_{ASE} is the ASE power measured in the bandwidth B_o, h and υ are Planck's constant and the optical frequency, respectively. An NF_{eq} improvement of more than 7 dB can be achieved.

High-power pump modules based on InGaAs/InP semiconductor diode lasers are available in the 14xx nm range. To reach higher powers, a combination of such diodes is necessary and this can be achieved with polarisation beam combiners. Two orthogonal pumps at the same wavelength can be combined with low loss to reach 700 mW of output power. The efficiency of such diodes is about 0.3 W/A taking into account the chip efficiency and the coupling efficiency.

A Raman Fibre Laser (RFL) is an all fibre technology. High output powers above 2 W can be achieved without difficulties with a single high-power and high-brightness laser source (developed in BRIGHTER) that is used to pump a fibre laser around 1.1 µm. A Raman resonator converts the 1.1 µm wavelength into any wavelength between 1200 nm and 1600 nm. The resonator uses the Raman effect in non-doped fibre to create gain at the Stokes wavelength. High reflectivity Fibre Bragg Gratings (FBGs) allow the laser effect in this fibre to concentrate the power in the cavity. In this way, the Raman effect occurs with high a conversion efficiency. By cascading several couples of FBGs, the power is converted step by step to a longer wavelength. The final step has a low reflectivity FBG in order to extract the majority of the power from the cavity at the desired wavelength. The power efficiency is lower than all semiconductor technology, but higher powers can be reached at a lower cost.

Application of Raman Amplification for WDM Systems

In an amplified transmission system, Erbium Doped Fibre Amplifiers (EDFAs) compensate the fibre losses. EDFAs are so-called lumped amplifiers as the gain is lumped at periodical points along the transmission line.

On the other hand, distributed amplifiers, such as Raman amplifiers, maintain the optical signal level during propagation. The counter-pumping configuration is adapted to to compensate for the signal losses along the transmission line. The co-pumping configuration allows for the launched signal power to be reduced, which minimises the impact of the non-linear effects along the transmission optical fibre as shown in Fig. 4. This is a strategic point to be considered for the future deployments of terrestrial 40 Gb/s WDM systems or very long-haul submarine systems.

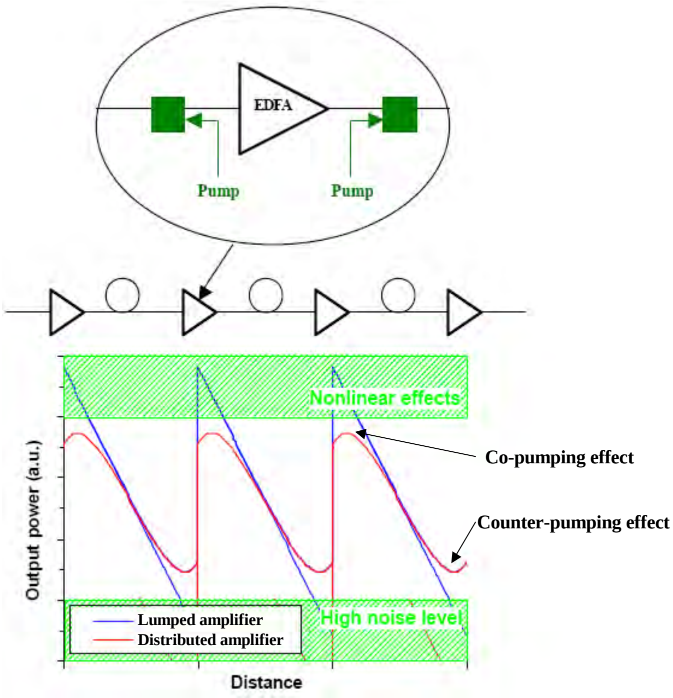

Fig. 4 (opposite): Comparative schematic diagrams of a lumped amplifier and a distributed amplifier.

The principle issues concerning DRA for WDM applications are [2]:

Multi-Rayleigh Scattering

The long interaction length of a Raman fibre amplifier gives rise to Rayleigh backscattering. The same process applies to the backscattered signal that gives rise to double Rayleigh backscattering (DRBS). This double Rayleigh portion serves as noise for the original signal. In the limit case of high gain, the DRBS introduces multi-path interference of the signal that may further degrade the system performance.

Polarisation Dependence

Because of long interaction length of Raman amplification, the polarised signal does not keep its polarisation state all along the fibre. If the pump is polarised, there are instabilities on the signal power because of the polarisation Raman gain dependence. To avoid this problem, semiconductor pump sources are combined in orthogonal polarisations in order to cancel their effect. Another way is to use a depolariser, but this increases the cost of the system. With a RFL, the pump has a very low degree of polarisation and the Raman gain does not change along the fibre.

Relative Intensity Noise (RIN) Influence

Co-propagating and counter-propagating Raman schemes can be used to amplify a signal. Semiconductor or Fibre Raman Laser have substantial intensity noise, which can be transferred to the signal. The Raman effect is a fast process (fs range). In a co-pumped Raman amplifier, the pump and signal propagate at slightly different velocities and therefore will “walkoff”. The walkoff is a function of the dispersion of the transmission fibre and will average the transfer of the noise from the Raman pump to the signal. In a counter-pumped Raman configuration, the noise from the Raman pump will be averaged over the transit time of the amplifier and this is why the counter-propagated scheme is generally chosen. The typical maximum value for the relative intensity noise (RIN) of the source to avoid RIN transfer is about –120 dB/Hz for co-propagating amplifiers and –110 dB/Hz for the counter propagating scheme.

Multi-Wavelength Raman Pumping for WDM Amplification

For a given power, a single Raman pump wavelength can provide 3 dB of flat gain in a wavelength range of about 30 nm. In order to use the available pump power efficiently, all WDM channels should benefit from Raman gain in the same way. Multi-wavelength pumping allows one to extend the Raman gain bandwidth. The total gain profile of such amplifiers consists of a superposition of the contributions from each individual pump.

The maturity of 14xx nm pump laser diodes readily leads to the realisation of practical broadband Raman amplifiers for WDM applications. However, this implementation presents several disadvantages in terms of system reliability due to complex arrangements for the coupling of the different laser diodes into the transmission fibre. A polarisation-diversity architecture is also required to avoid polarisation Raman gain dependence. The induced loss impacts on the cost and on the electrical-to-optical conversion efficiency.

Alternative means consist of a multi-wavelength cascaded Raman laser source able to emit high power (>2 W). These Raman Fibre Lasers simultaneously emit randomly polarised light at several wavelengths from a single cavity. Figure 5 shows the architecture of the 3λ-RFL. The incident pump light is from an 1100 nm Yb-doped double cladding-pumped fibre laser, which is pumped by a single 975 nm or 920 nm high-power and high-brightness laser source (developed in BRIGHTER). A spool of single mode fibre, with four pairs of high reflective (HR) FBGs, shifts the wavelength from 1100 nm to 1347 nm. Another set of three high reflective – low reflective FBGs allows one to reach the specified wavelengths of 1428 nm, 1445 nm and 1466 nm.

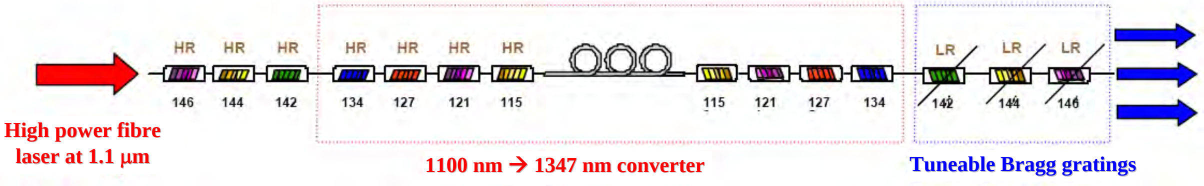

Fig. 5: Three-wavelength Raman Fibre Laser source architecture.

A voltage thermally controls the FBG reflectivity to adjust the output power for each wavelength. The output spectrum of the tuneable RFL exhibits eight spectral components (see Fig. 6). The first five wavelengths come from the residual powers of the successive Stokes waves generated in the cavities closed by HR Bragg gratings. The last three wavelengths correspond to the usable pump wavelengths for distributed Raman amplification in the transmission fibre. The total output power is distributed among the three wavelengths. By simple adjustment of the FBG voltages, up to 10 dB dynamic power range at each wavelength is achieved. Figure 7 shows the interdependence of the optical powers at the 3 different wavelengths with the tuning of the FBG_{1445nm} voltage. This behaviour is due to the unique laser cavity that acts as a unique energy reservoir. The only active component is the 975 nm or 920 nm high-power and high-brightness laser source for the 1100 nm Yb laser.

Distributed Raman amplification has been demonstrated over 20 km of dispersion shifted fibre using a counter propagation scheme. The Raman pump is a 3λ-RFL and the signal is a WDM 16-channel comb in the C-band (1529 nm - 1563 nm). To minimise the gain variation, the pump powers have been optimised to P_{1428nm} = 107 mW, P_{1445nm} = 92 mW and P_{1466nm} = 126 mW. Measurements are in good agreement with the numerical results (see Fig. 8). We obtain less than 1.5 dB gain ripple over the C-band. The control of the FBG reflectivities permits efficient dynamic gain adjustment.

Conclusion

The fundamentals of Distributed Raman Amplifiers for WDM transmission systems have been presented. It has been shown that flat broadband Raman gain can be obtained using multi-wavelength pumping. The 3λ-RFL is a simple configuration for providing high-power, multi-wavelength pump sources and is a pertinent alternative to multiplexed semiconductor laser diodes.

References

[1] R.H. Stolen and E.P. Ippen, “Raman gain in glass optical waveguides” *Appl. Phys. Lett.*, Vol. 22, No. 6, pp. 276-278, 1973.

[2] S. Namiki and Y. Emori, “Ultrabroad-band Raman amplifiers pumped and gain-equalized by wavelength-division-multiplexed high-power laser diodes” *IEEE J. Select. Topics Quantum Electron.*, Vol. 7, No. 1, pp. 3-16, 2001.

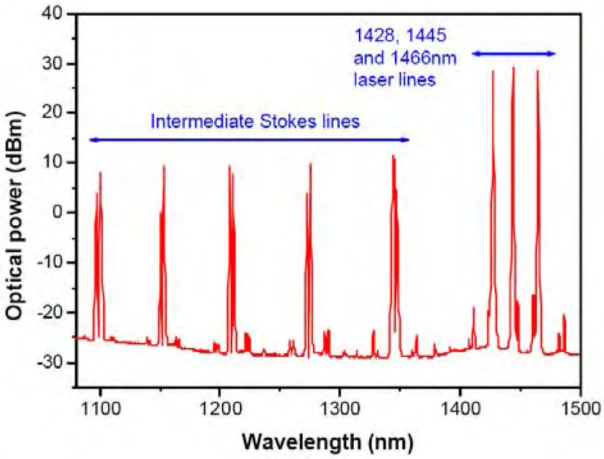

Fig. 6: Output spectrum of a 3λ-RFL with equalised power at the 3 output wavelengths.

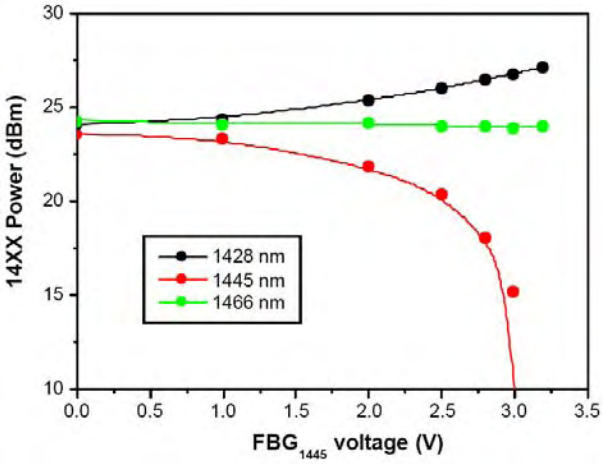

Fig. 7: Power evolution of the 1428 nm, 1445 nm and 1466 nm pumps versus the FBG_{1445nm} voltage. The FBG_{1428nm} and FBG_{1466nm} voltages are fixed at zero.

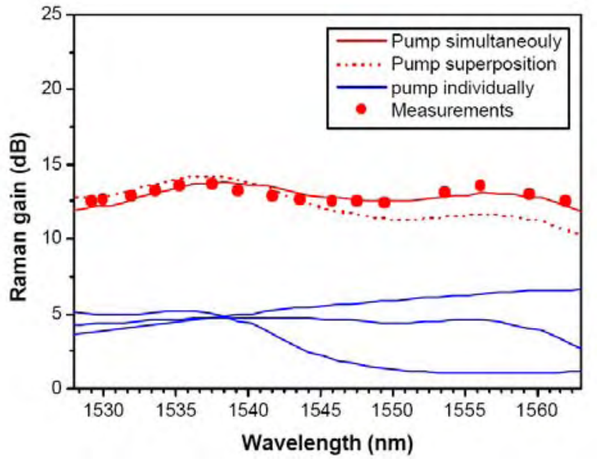

Fig. 8: Gain spectrum of a C-band Raman amplifier using the 3λ-RFL with P_{1428nm} = 107 mW, P_{1445nm} = 92 mW and P_{1466nm} = 126 mW injected into 20 km of dispersion shifted fibre (lines – numerical results, dots – measurement results).

Diode Laser Sources for Display Applications

M. Reufer, M. Schmitt, P. Brick and N. Linder

OSRAM Opto Semiconductors GmbH

Leibnizstr. 4, 93055 Regensburg, Germany

N. Collings, R.V. Penty and B. Crossland

Electrical Engineering Division, Department of Engineering, University of Cambridge

9 JJ Thomson Avenue, Cambridge, CB3 0FA, U.K..

Motivation

In the recent years, mobile devices like cell phones, personal media players and digital cameras have become more powerful, enabling them to handle high resolution images and video sequences. Simultaneously with increasing technical progress, the devices are getting smaller and smaller. This progress leads to a significant reduction of the available display size, which is typically limited to a standard resolution of 320 x 240 pixels on a 4 inch diagonal screen. This imbalance between ubiquity of information and entertainment and the limited display capabilities demand for innovative display concepts which overcome the physical size of the handheld electronics. Different ideas like foldable displays based on organic materials have been discussed but are still far away from becoming a product for the consumer market. In general, projection displays are able to produce images with relevant image diagonal, but the established technologies are based on rather bulky light sources which make them too space and power consuming to become a real battery operated mobile device.

Display Systems

One step towards mobile projector displays has been made by using LEDs as light sources in display applications. The first portable LED projectors appeared on the market in recent years. Image generation in LED based devices are made either by homogeneous illumination of a LCD or LCoS or by focusing the divergent light of the different coloured LEDs on a moving mirror array.

Both of the above concepts have technological drawbacks. The use of a LCD or moving mirror array for image generation induces losses because a significant amount of light is blocked and not delivered to the projected image, thereby reducing the overall efficiency. Efficient collimation of the diverging light output of LEDs demands for sophisticated and expensive optics. One key issue for the mobile applications in general is to provide highly efficient devices which enable long lasting operation times within a battery cycle.

The output power of today's portable LED projectors restricts the application either to small display sizes or to operation under reduced ambient light conditions. Projection schemes based on laser diodes have the capability of providing brighter light sources, opening the path towards more ubiquitous display applications.

One focus of the WWW.BRIGHTER.EU project is the development of suitable laser sources as an enabling technology for high brightness projection displays. Two technology routes for laser projection displays are being explored and these are described in the following sections.

1. Projection Displays using Scanning Mirror Technology

One concept of display generation based on laser sources is the flying-spot scheme illustrated in Fig. 1. The output of three different laser sources (blue, green and red) is overlaid by dichroic optical elements and is collimated onto a single scanning mirror. The micro-machined mirror moves at high speed, writing the image pixel by pixel, analogous to the function of the conventional cathode ray tube. The colour and brightness of each pixel is defined by the intensity of the three different laser sources.

One of the advantages of such a projection system is the infinite depth of focus inherent to high brightness laser sources. This feature allows for direct projection on non-planar surfaces, making applications like head-up displays in automobiles possible.

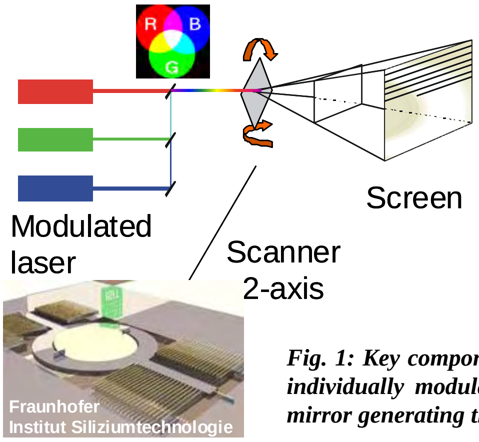

Targeting the market of mobile applications like micro-projectors or head-up displays requires display sizes of about 40cm in diagonal in order to address the key markets for high volume products. An established requirement for display luminance is around 700cd/m^2, enabling satisfactory image quality of the projector even at elevated ambient light levels. In order to achieve this luminance and to cover a wide colour gamut, laser output powers of several 100 mW per colour are needed from laser sources providing good (nearly diffraction limited) beam quality.

Fig. 1: Key components of a scanning mirror based laser display. The outputs of the three individually modulated lasers are coupled co-linear onto a fast moving scanning micro-mirror generating the image by subsequent writing of individual pixels.

Technical Approach

A flying-spot projection scheme requires high brightness lasers since the pixel size on the screen is defined by the laser spot size. The choice of a suitable laser concept depends on the colour. Blue and red emitting laser diodes with good beam quality and adequate output power can be realised as edge emitting lasers (either as ridge waveguide or as tapered lasers). In contrast, green laser sources cannot be realised as direct-emitting single-mode lasers. Neither the InAlGaP nor the InAlGaN material system offer direct green laser sources. Instead one has to rely on IR-sources and a frequency doubling scheme. High beam quality is necessary from the IR source to enable high conversion efficiency.

The lasers have to be capable of fast modulation of the optical output. For a display with a resolution of 1024 x 768 pixels and an image frequency of 100 Hz the pixel frequency results in 100MHz. The rise and fall times of the lasers have to be even faster. In principle, it may be possible to control the analogue output level by external components like electro-optical or acousto-optical modulators. However, these external components raise complexity, size and price of any system. In contrast, direct modulation of the laser source with its small form factor and simple alignment is certainly preferred.

The technical scope of the Brighter consortium is to realise lasers combining output power of several 100mW with nearly diffraction limited beam quality, with a special focus on the realisation of red and green lasers.

Red lasers sources can be realised as direct emitting lasers on the material system InAlGaP. The choice of the exact wavelength is dominated by two factors. Firstly, the sensitivity of the human eye increases strongly at shorter wavelengths, which in general reduces the optical output power needed to achieve a bright optical impression. On the other hand, the electro-optical efficiency of red lasers drops for shorter wavelengths due to an increased electron leakage in the semiconductor material. The trade-off between these two factors leads to 650nm as the wavelength of choice.

Since state of the art ridge-waveguide lasers are limited by catastrophic optical damage, the red lasers will be realised as tapered lasers. In addition to the output power of ~600mW, a fast modulation speed of 100MHz is required to enable image generation with XGA resolution. This high modulation speed will be achieved by separate contacts for the ridge and the taper section of the laser. This approach allows for keeping the taper section at a constant bias while only the ridge section is modulated at high speed.

In order to enable efficient heat dissipation from the laser, p-side-down mounting is necessary. This requires a special segmented heatsink where the ridge and taper can be biased separately.

In contrast to red, green laser sources cannot be realised as direct emitting lasers. Therefore, one has to resort to IR-sources emitting around 1060nm and a frequency doubling scheme. Again an IR-ridge waveguide can in principle provide the required high beam quality, but is limited in output power due to COD. As a consequence, one has to rely on an IR tapered laser concept as the pump source for the second harmonic generation.

In general, frequency doubling is considered to be most efficient in external cavity approaches. However, single pass frequency doubling is superior from a manufacturing perspective due to a reduced complexity and small form factor. Since substantial progress has been made in improving the single pass conversion efficiencies in periodically poled Mg-doped lithium niobate (more than 10%), this concept is being explored.

Another prerequisite for an efficient second harmonic generation is a stable infrared wavelength, which makes a stable wavelength selection of the IR source essential. Two approaches for wavelength stabilisation are being tested for feasibility within Brighter. Both integrating a DFB grating in the ridge of the IR tapered laser as well as an external grating at the antireflection coated ridge can serve as wavelength selection tools. While the first demands for more sophisticated semiconductor processing steps, in the second case an additional external optical element has to be aligned to the ridge of the tapered laser.

Fast modulation of the green laser source can be realised by modulating the ridge section of the IR tapered laser, in the same manner as with the red tapered laser. Based on this approach, high modulation frequencies of IR tapered lasers have already been shown by the project partners [1].

2. Projection Displays using Computer Generated Phase Holograms

The Photonic and Sensors Group at the University of Cambridge, in an activity led by Professor Bill Crossland and Dr Neil Collings, have been developing a novel form of projection display based on phase holograms. The Fourier transform of the desired 2D image is programmed onto a phase-modulating Liquid Crystal on Silicon (LCOS) microdisplay. When illuminated by a set of RGB lasers, a full colour image is projected from a very compact unit (see Fig. 2).

The first device based on a phase hologram that could be used for projection display was the Eidophor [2]. An oil film is deformed by a cathode ray beam to produce the phase profile and a Schlieren system is used to convert the phase image into an amplitude image. Schlieren optics result in light loss because the light diffracted out of the beam path is deposited on the bars of a mirror bar system. A more efficient phase structure is one where the light is re-directed from the dark parts of the image into the illuminated parts. This is performed by more complex phase screens than the ones used in the Eidophor system.

Fig. 2: Miniature Projection Display Concept.

The phase only Fourier hologram is computed using iterative techniques based on the Gerchberg Saxton algorithm [3]. For real time video images, there is a significant computational overhead since the hologram needs to be computed at the frame rate. Until recently, this was not possible at reasonable cost. However, developments in speed and complexity mean that specialist digital processing hardware that computes the phase hologram in real time is now possible.

The Display Device

The key component which spatially modulates the phase of the light beam is called a spatial light modulator. The device that we use is a nematic liquid crystal on silicon integrated circuit (LCoS), which was initially researched in the 1970s [4]. Other devices can be used such as those based on piston MEMS, such as the Grating Light Valve. We currently use an HDTV LCoS device from Holoeye Photonics AG which produces 2π phase modulation in the visible region.

Figure 3 shows three approaches to making a hologram for a simple task such as focussing a collimated light beam. The Fresnel zone plate (FZP) is a binary amplitude screen composed of absorbing and transmitting zones which produce a diffraction pattern along the optical axis. Approximately 10% of the incident light goes into the primary focus. The Phase zone plate is a binary phase screen with no absorbing zones. The alternating zones of 0 and π phase delay can be viewed as the sum of the transmitting zones of two FZPs, so that the resulting amplitude efficiency in the primary focus is twice that of the FZP. Therefore, the intensity efficiency is four times, or 40%. The Phase Fresnel Lens is an analogue phase screen which is a modulo 2π equivalent to a plano-convex lens which will produce up to 100% efficiency at the focus of the lens.

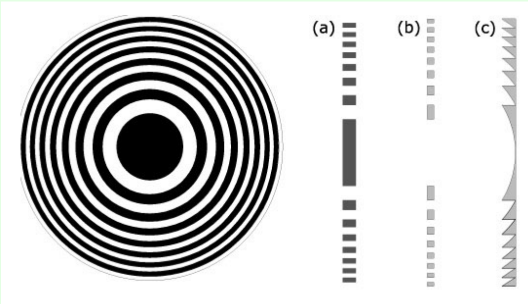

Fig. 3: (a) Fresnel Zone Plate; (b) Phase Zone Plate; (c) Phase Fresnel Lens.

Advantages of Phase Projection

In addition to the efficiency advantage due to the redistribution of light in the image plane, there is a further efficiency advantage due to the use of polarised solid state light sources. Three, R,G and B, sources provide a rich colour gamut with no requirement for an absorbing colour wheel or polariser.

Moreover, display brightness is promoted by using a small display device due to the Fourier transform relationship between the hologram plane and the replay field. This is the opposite situation to conventional projection displays where the etendue consideration obliges the manufacturers to maintain a reasonable area for the display device. Small device area reduces silicon real estate and costs of volume production.

Reduced pixel size is also avoided in conventional displays because it leads to proportionally larger pixel gaps which reduces the cosmetic display quality. In phase projection, the gaps between the pixels in the replay field are controlled by the degree of tiling in the hologram plane. Small device pixels increase the hologram resolution and strengthen fringing fields, which may improve the overall phase response.

The effect of quantisation in the hologram plane is shown in Fig. 4. The quantisation noise is redistributed throughout the replay field so that the quantisation noise is no longer visible compared with the amplitude quantised image. Similar considerations apply in the case of “dead” pixels due to faults in the display device, so that yield margins on display devices are improved when they are used for phase projection.

Further benefits are the frame-by-frame averaging of the noise field and the software control of replay field aspect ratio.

Fig. 4: Projected images from an amplitude screen that has been discretised to 4-bit grey levels (top) and from a phase screen discretised to 4-bit phase levels (bottom).

Early Results

We have constructed an prototype display using an LCoS device in which the phase image reflected from the device is propagated through a lens onto a screen (see Fig. 5). The replay field (see Fig. 6) shows good registration of the three colours despite the fact that only a single projection lens is used. This attests to the versatility of holograms that can be individually tuned to generate a colour display.

Cambridge will use the high brightness lasers being developed in the BRIGHTER project to improve the image quality and brightness.

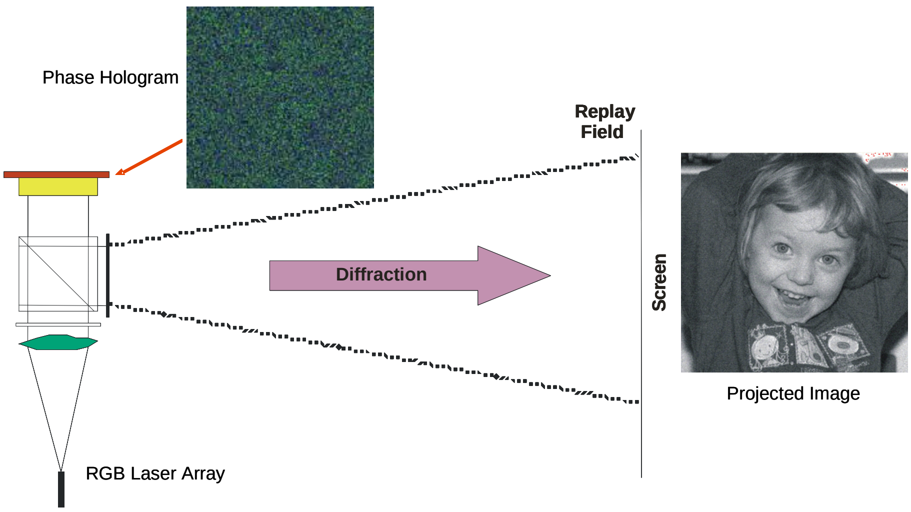

Fig. 5: Projection Display Prototype.

Fig. 6: Replay field of hologram using R,G and B lasers.

Market Potential

The main market is naturally in the area of all hand-held / mobile devices such as cell phones, portable media players and also laptop computers. It can be expected, that the first pocket projectors will be so called companion devices. They will have the size of a small cell phone, have its own power supply (battery) and be connected to the hand-held device by wire or wireless. A market entry of companion devices can be expected in significant quantities in the 2009 time frame.

In a second step, such projectors will be integrated into the hand-held / mobile device itself. This means the projector will use the power supply of the hand-held device. The expected market entry will probably be in 2010. This second step will also further improve or even enable new applications for hand-held devices like mobile TV. Together with the companion projectors, market studies (e.g. from Inside Media) predict up to 30 million projector units in 2012.

Projection displays would not only provide a solution to the hand-held / mobile device market but would also enable solutions within the automotive area (e.g. head up displays, HUD) since such projectors would provide significant advantages in regards to efficiency, contrast, brightness and form factor. With alternative mounting inside the car such projectors would pave the road to a significant after market and would support the penetration of HUDs into middle class vehicles. This would mean that the current market of 10,000-100,000 HUD units per year can be increased substantially.

Conclusion

Projection displays based on lasers as light sources show a substantial potential for future mobile applications. High efficiency together with the brilliance supported by the tapered laser concept is a key advantage versus other technical approaches.

References

[1] C.H. Kwok, R.V. Penty, I.H. White, K.-H. Hasler, B. Sumpf and G. Erbert, “Twin-contact high brightness tapered laser for high modulation efficiency high speed signal modulation” Submitted to 8th Asia-Pacific Optical Communications Conference (APOC 08), to be held 26th – 30th October 2008, Hangzhou, China.

[2] http://www.earlytelevision.org/yanczer_eidophor.html - The history of the Eidophor is outlined and complemented with informative sketches of the principle of operation. Accessed 21 December 2007.

[3] R.W. Gerchberg and W.O. Saxton, “A practical algorithm for the determination of phase from image and diffraction plane pictures”, Optik 35 (1972) 237-246.

[4] W.A. Crossland, P.J. Ayliffe and P.W. Ross, “A dyed-phase-change liquid-crystal display over a MOSFET switching array”, Proc. SID 23 (1982) 15-22.

Overgrowth Free High Power Single Mode Lasers

M. Kamp, P. Weinmann, C. Zimmermann, W. Kaiser, and A. Forchel
Technische Physik, Universität Würzburg, Am Hubland, 97074 Würzburg,Germany

1. Introduction

An increasing number of applications requires single mode lasers or lasers with a narrow emission spectrum in combination with the capability to deliver high output powers. Examples are frequency doubling of infrared lasers or lasers for solid state or fibre laser pumping. The demand for high output power in combination with a good beam quality can be met by tapered laser diodes [1,2]. However, no frequency selection is provided in standard tapered lasers and the emission spectrum is comprised of several longitudinal modes, leading to a typical spectral width of a few nm. This article describes several approaches towards high power single mode laser sources with an emphasis on overgrowth free fabrication technology. The second section gives a brief review of single mode lasers with small to medium output powers realised by overgrowth free fabrication technologies. The third section discusses how some of these concepts can be applied to tapered lasers. Section four describes the fabrication of the devices. Characterisation results of the various devices types are then presented in sections five to seven.

2. Overgrowth free single mode lasers

The traditional way to realise a single mode semiconductor laser is the incorporation of a frequency selective element in the laser cavity. This element leads to a discrimination of the preferred laser mode with respect to all other modes by decreasing the threshold gain of the laser mode and/or by increasing the threshold gain of the undesired competing modes. Structures which are commonly used are based on feedback gratings which are either placed the end of the laser resonator in order to realise a wavelength selective reflector (distributed Bragg reflector, DBR) or along the laser cavity (distributed feedback laser, DFB). In case of the DFB laser, the feedback gratings can couple to the optical mode either via a modulation of the refractive index (index coupled DFB) or the gain (gain coupled DFB). The latter are sometimes also called complex coupled DFB lasers since a modulation of the gain usually involves a modulation of the refractive index as well.

One of the major applications of DFB lasers is their use as light sources for wavelength multiplexed optical fibre links where each transmission channel is carried on a separate wavelength. The output power of these devices is typically on the order of a few to a few tens of milliwatts. The standard way to fabricate these DFB lasers is based on multiple epitaxial steps. The growth of the laser layer is interrupted in the upper cladding layer, a grating is formed by lithography (usually a holographic exposure of photoresist) and etching, and the growth of the laser is completed in a second epitaxial step. This technology is very well established for InP based materials, but the transfer to other material systems is not straightforward. Aluminium containing layers, which are used for GaAs based laser diodes in the 1 µm region, pose a challenge due to the formation of oxide layers on the surface. Consequently, a number of fabrication schemes for single mode lasers without any regrowth steps have been investigated. In this case, the grating is not incorporated in the layer structure, but placed on the top of the waveguide, lateral to it, or at the front or back of waveguide. In the first two cases, the device would be a DFB laser since the grating extends over the entire length of the laser and the last case corresponds to a DBR laser. In all three cases, the grating can be defined after the growth of the laser structure is completed.

DFB lasers where the grating is placed on top of the ridge waveguide (RWG) are discussed in [3,4]. A metal grating was used, which resulted in a complex coupled DFB laser. In order to achieve sufficient overlap between the optical mode and the grating, the thickness of the upper cladding layer had to be reduced compared to a standard laser structure. Recently, this concept has been used for the realisation of single mode quantum cascade lasers [5]. Several configurations are possible for a lateral grating. The grating can either be defined on the sidewalls of an (etched) ridge waveguide [6] or lateral to the latter. Devices with an etched sidewall grating are attractive since the lithography of the grating is carried out on a planar surface, allowing the use of imprint lithography. The advantage of imprint compared to a holographic exposure of the grating is the flexibility of the grating definition (e.g. free choice of grating periods). On the other hand, imprint is difficult on non-planar surfaces. If a lateral grating is used, it can either be etched into the semiconductor, resulting in an index coupled DFB laser [7], or it can be defined by metal evaporation and lift-off, leading to a complex coupled device [8]. Index coupled DFB lasers have been realised on GaAs [9] and InP [10] based laser structures, the approach based on lateral metal grating has been applied to a wide variety of laser structures [11-15]. Finally, it is possible to place the grating at the end of the waveguide. In this case, the DBR grating acts as a highly reflective mirror [16].

There are also ways to achieve single mode lasing without the use of a grating structure, e.g. by a combination of two cavities with slightly different length [17]. Due to the difference in length, the Fabry-Perot mode combs of both cavities have a slightly different spacing. If designed correctly, there is only a single coincidence of modes from either cavity within the gain spectrum of the active region, resulting in single mode laser emission. Initially, the coupled cavities were realised by cleaving the laser and soldering the two pieces in close proximity on a submount. More recent implementations use an etched on-chip reflector to define the two cavities [18]. A rather sophisticated version of these Fabry-Perot based devices are the so called 'discrete mode lasers' [19], where several small perturbations of the refractive index are introduced along the laser waveguide, resulting in single mode emission.

3. Single mode tapered lasers

The output powers of the devices discussed above are limited to a few tens of mW, usually by thermal effects. In order to realise higher output powers, a ridge waveguide can be combined with a tapered amplifier which boosts the power to several Watts. The ridge waveguide acts as a mode filter in these devices, so that properly designed devices deliver not only high output powers, but also a good beam quality and therefore high brightness.

In order to obtain single mode emission, frequency selective elements like the ones discussed above have to be included into the devices. Fig. 1 shows schematics of the three different approaches discussed in this paper. In all cases, a ridge waveguide with a frequency selective element is combined with a tapered amplifier. In the device shown in Fig. 1a, a DFB section with lateral gratings is used for mode selection. Fig. 1b shows a device based on a wavelength selective reflector (DBR) at the end of the ridge waveguide. The device depicted in Fig. 1c uses a combination of two cavities with different length. In all devices, a gain guided taper is used, with a typical opening angle of 6º. The light is emitted from the AR coated front facet.

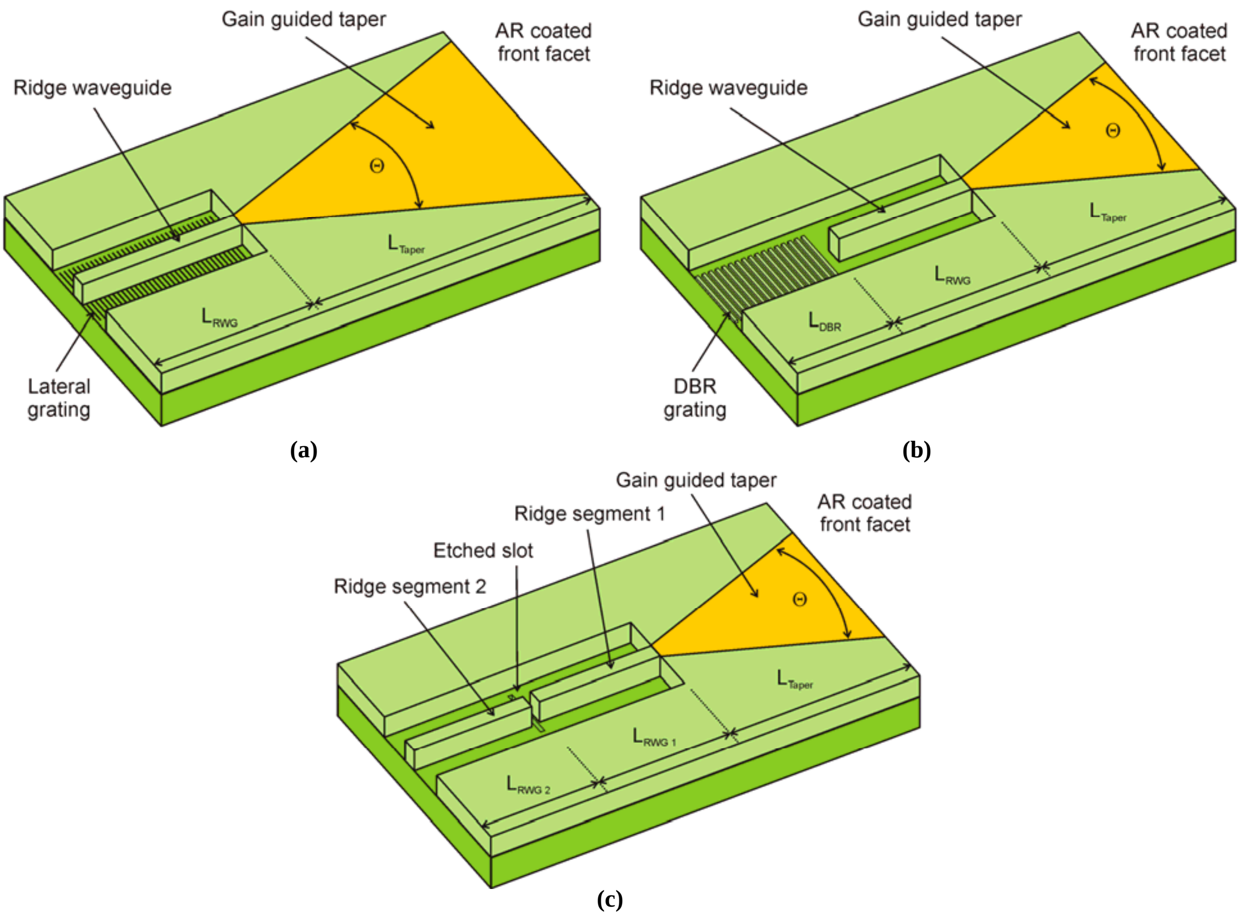

Figure 1: Schematics of the three different design approaches: (a) DFB based tapered laser, (b) tapered laser with DBR, (c) coupled cavity tapered laser.

When these approaches are applied to high power lasers, several issues have to be kept in mind. First of all, the vertical waveguide of high power lasers is typically based on large or even super-large optical cavity structures in order to reduce the facet load and decrease the vertical far field angle. This leads to a concentration of the optical mode in the waveguide layer, and the overlap of the mode with cladding layer is consequently reduced. This can reduce the coupling to the DFB or DBR gratings used in Figs. 1a and 1b. In addition, the introduction of frequency selective elements in the laser can lead to additional losses, so a slight increase of the threshold current and a reduction of the efficiency are expected in this case.

4. Fabrication

The first process step for all device types (Figs. 1a to 1c) is the definition of the ridge waveguides by optical lithography. After development of the photoresist, a BaF_2/Cr etch mask is evaporated and lifted-off. Subsequently, the ridges are formed by an electron-cyclotron-resonance reactive-ion-etch (ECR-RIE) process. The length of the ridge waveguides is typically around 1 mm, while the width and depth have to be designed to match the diffraction angle of the ridge waveguide mode with the opening angle of the taper. For the DFB and DBR based devices, the grating is now defined by high-resolution electron beam lithography at the corresponding position. The emission wavelength λ and the grating period Λ are related by Bragg's formula:

$$\lambda = 2n_{eff}\frac{\Lambda}{m}$$

where n_{eff} is the effective refractive index of the laser waveguide and the integer number m denotes the order of the grating. For the InGaAs/AlGaAs devices described in this paper, the effective refractive indices are between 3.2 and 3.3. For devices emitting around 1 µm, this translated into a grating period of about 150 nm for first order and 300 nm for second order gratings.

After development of the E-beam resist, chromium is evaporated, followed by a lift-off process. In the case of a DFB laser with lateral grating, the definition of the grating is finished at this stage. Fig. 2a shows a scanning electron microscopy (SEM) image of a ridge waveguide with a lateral Cr grating. The large picture shows a second order grating, a first order grating is shown in the inset. It is important to have the grating lines extend all the way to the ridge, since the field of the guided mode decreases exponentially outside the ridge. A gap between the ridge and the grating would therefore lead to a substantial decrease of the coupling efficiency. In case of the DBR devices, the Cr is used as an etch mask for the subsequent dry etch step that transfers the grating into the upper cladding layer. Fig. 2b shows the rear end of the ridge waveguide and the etched DBR grating. The typical etch depth is around 200 nm. For devices based on coupled cavity structures, a deep trench is etched between the two waveguides using a SiO_2 etch mask. Then the samples are planarised by spin-coating a layer of benzo-cyclobutene (BCB). Next, the taper sections with opening angles of typically 6° and lengths between 1 and 3 mm are defined by optical lithography. The removal of the highly conductive GaAs contact layer outside the taper region by wet etching forms the gain guided taper. A MgO layer is evaporated for additional isolation, followed by deposition of the p-contacts. Finally the sample is thinned and a n-contact layer is evaporated and annealed.

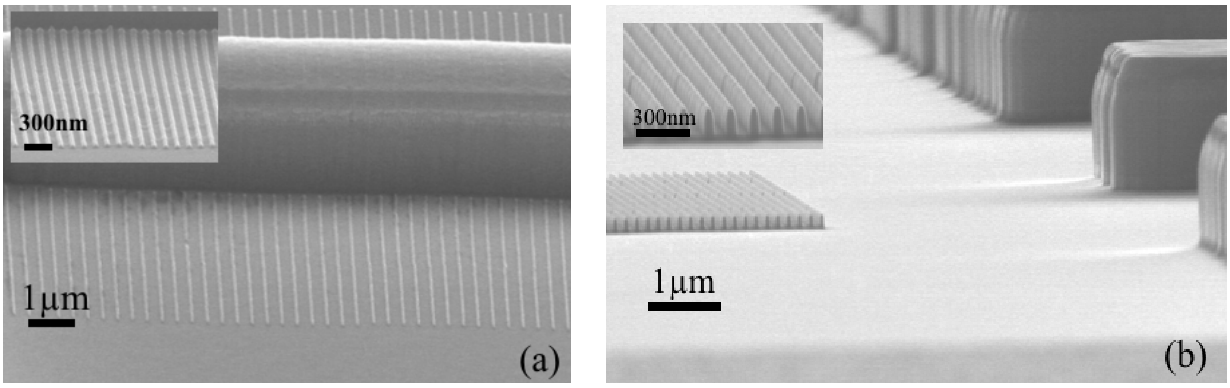

Figure 2: (a) SEM image of a lateral chromium grating next to the ridge waveguide, (b) SEM image of a DBR grating at the end of the ridge waveguide. The insets show images of the gratings at higher magnification.

After cleaving the devices, facet coatings are applied. An anti-reflection coating is deposited on the front facet of all devices. In case of the DFB laser, a high-reflection coating is deposited on the rear facet. This is not required for the DBR devices, where the grating acts as a reflector.

5. Tapered lasers with lateral feedback grating

The laser structure used for the device described here is an InGaAs/AlGaAs quantum dot laser grown by molecular beam epitaxy. It uses a single layer of InGaAs/GaAs quantum dots emitting around 920 nm as the active region. The quantum dot layer is embedded in a 600 nm wide graded index separate confinement heterostructure (GRINSCH). The Al content of this AlGaAs GRINSCH is varied between 40 and 60%. It is surrounded on both sides by 1600 nm thick $Al_{0.6}Ga_{0.4}As$-cladding layers. The structure is capped with a highly p-doped 150 nm thick GaAs layer. The internal parameters of the laser structure were determined by measurements of 100 µm wide broad area lasers, yielding a transparency current density of 190 A/cm^2, an internal quantum efficiency of 71% and an internal absorption of 2 cm^{-1}. Tapered lasers with lateral DFB gratings were fabricated using the process described above [20].

Fig. 3a shows the light output characteristic of a device with a 1 mm long ridge waveguide and a 2 mm long taper section with an opening angle of 4º. The grating period of the first order lateral grating was 143 nm. The laser has a threshold of 351 mA, which corresponds to a threshold current density of only 250 A/cm^2. The slope-efficiency is 0.51 W/A, leading to an output power of more than 500 mW at a drive current of 1500 mA. As a reference, a tapered device without a grating was measured. It has a comparable threshold current of 335 mA, but a higher slope efficiency of 0.70 W/A. This difference is caused by the additional absorption introduced by the lateral grating. The emission spectra of the device for three temperatures are shown in Fig. 3b. The measurements were performed at twice the threshold current. At room temperature, the laser emits at 924 nm. Increasing the sub-mount temperature to 80°C shifts the emission to 928 nm. The side mode suppression ratios (SMSR) are between 30 and 40 dB. The DFB emission is located on the long wavelength side of the gain spectrum at room temperature (red curve in Fig. 3b). As the operation temperature is increased, the peak of the material gain shifts towards and through the emission line. Due to the initial detuning and the small shift of the QD emission with temperature [21], stable basic characteristics with temperature are obtained. Up to 70°C, a nearly constant power slope of 0.5 W/A together with an only slight increase of the threshold current is achieved. Measurements of the beam caustic were used to determine the beam quality factor M^2, which stays well below 1.3 up to drive currents of 1.5 A.

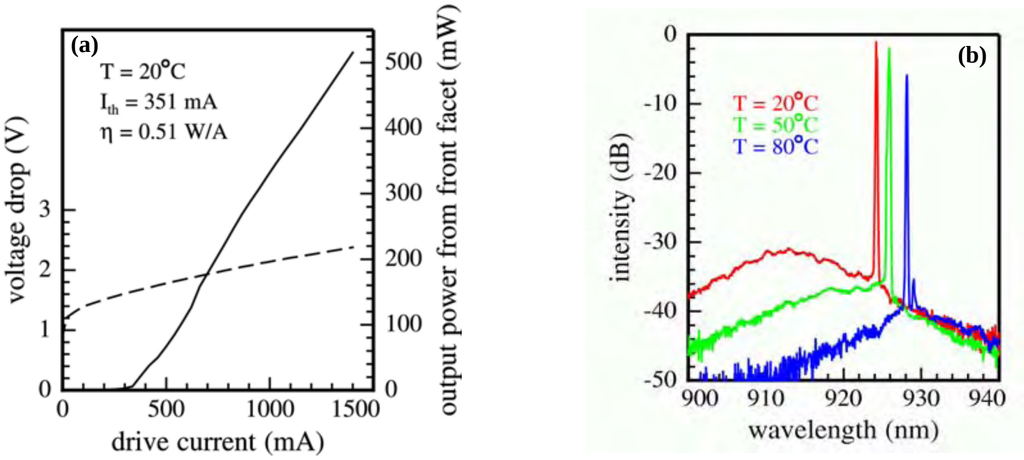

Figure 3: Device characteristics of a QD tapered laser diode with lateral feedback grating. a) Light output at the front facet. The threshold current is 351 mA and the slope efficiency 0.51 W/A. A maximum output power of 500 mW is reached. b) Emission spectra of the device at three different temperatures.

At drive currents larger than 1.5 A, the emission of the device becomes unstable and additional modes show up in the emission spectrum. The reason is the rather small coupling coefficient of the grating. As discussed in sections 2 and 3, the grating couples to the evanescent part of the laser mode. Increasing the thickness of the optical waveguide leads to an expansion of the mode and a concentration of the optical power in the core of the waveguide, with a corresponding decrease of the intensity in the cladding layers. Even for the moderate thickness of the GRNISCH used here (600 nm), the coupling coefficient of the lateral grating is quite small, which compromises the suppression of unwanted modes at high output powers.

6. Tapered lasers with DBR section

The second approach for high power single mode lasers to be discussed are tapered lasers with a Distributed Bragg-Reflector (DBR) for frequency selection. In this case, the DBR grating at the end of the ridge waveguide acts as a frequency selective reflector. The layer structure used for the fabrication of the devices is similar to the one used for the DFB devices. The DBR grating has a length of 0.8 mm, the ridge waveguide section has a length of 1 mm and the taper has a length of 1.4 mm, resulting in a total device length of 3.2 mm. Since the DBR grating is much closer to the optical mode than the lateral DFB grating, a larger coupling coefficient and an increased stability of the single mode operation is expected.

Fig. 4 shows the device characteristic of the tapered lasers with DBR grating. The output power characteristic is plotted in Fig. 4a. The laser has a threshold current of 400 mA and a slope efficiency of 0.61 W/A. A maximum single mode output power of 1 W is reached at a drive current of 2 A. Fig. 4b shows the emission spectrum of the device, which is single mode with a sidemode suppression ratio of around 45 dB.

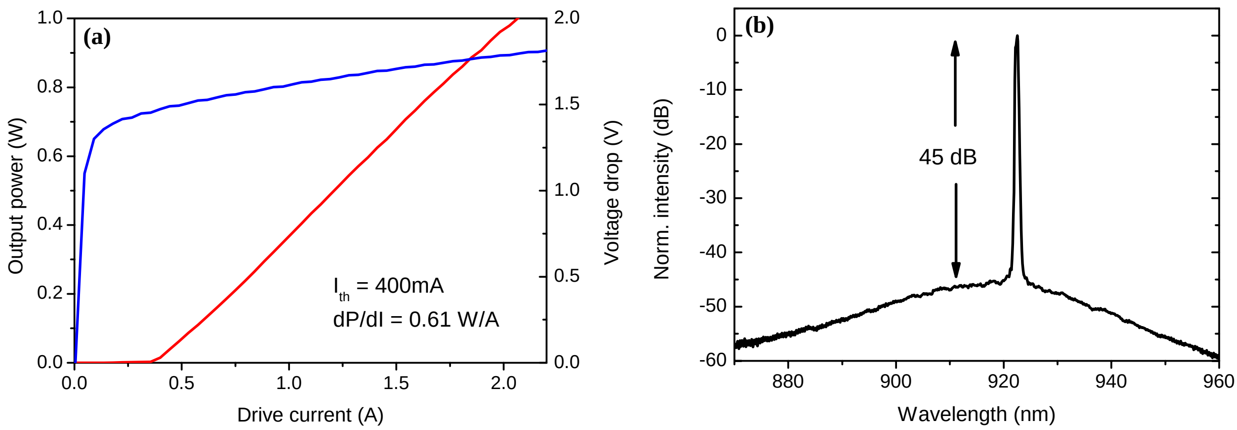

Figure 4: Device characteristics of a quantum dot tapered laser diode with DBR grating. a) Light output characteristic. The laser has a threshold current of 400 mA and a slope efficiency of 0.61 W/A. The maximum single mode output power is 1 W. b) Emission spectrum of the device. Single mode emission with a SMSR of 45dB is obtained.

The far field angles of the laser at $1/e^2$ are 48° in the fast axis and 8.2° in the slow axis. In order to determine the beam quality factor M^2, the radius of the beam waist was measured as a function of the distance from a focussing lens. The results are plotted in Fig. 5a. For output powers below 1 W, M^2 is almost constant and below 2.

One advantage that is common to all approaches that include a grating is the temperature stabilisation of the emission wavelength. In devices without wavelength selective elements, the emission wavelength is determined by the gain curve of the active region. Temperature changes will results in changes of the emission wavelength due to changes of the bandgap in the active region. If the laser is used in applications where the emission wavelength has to be within a narrow spectral region (e.g. when pumping solid state lasers with narrow absorption bands), an accurate stabilisation of the laser temperature is required to maintain the emission within the target values. This effect can be reduced by the use of quantum dots in the active region [21], but an even better stabilisation is achieved in the lasers with gratings. In this case, the shift of the emission is determined by the temperature dependence of the refractive index.

Fig. 5b shows the emission wavelength of a quantum dot based tapered laser with and without grating. The emission of the device without grating shows a shift of 0.2 nm/K, which is already smaller than the shift of a corresponding quantum well device (0.3 nm/K). The wavelength shift of the laser with grating is reduced to 0.08 nm/K. In combination with the small wavelength shift of the quantum dots, this can be used to compensate the decrease of laser performance at elevated temperatures. If the emission wavelength of the DFB/DBR is designed to be on the long wavelength side of the gain spectrum at room temperature, the gain peak will shift slowly towards the emission wavelength with increasing temperature, resulting in a stable laser performance over a wide temperature range.

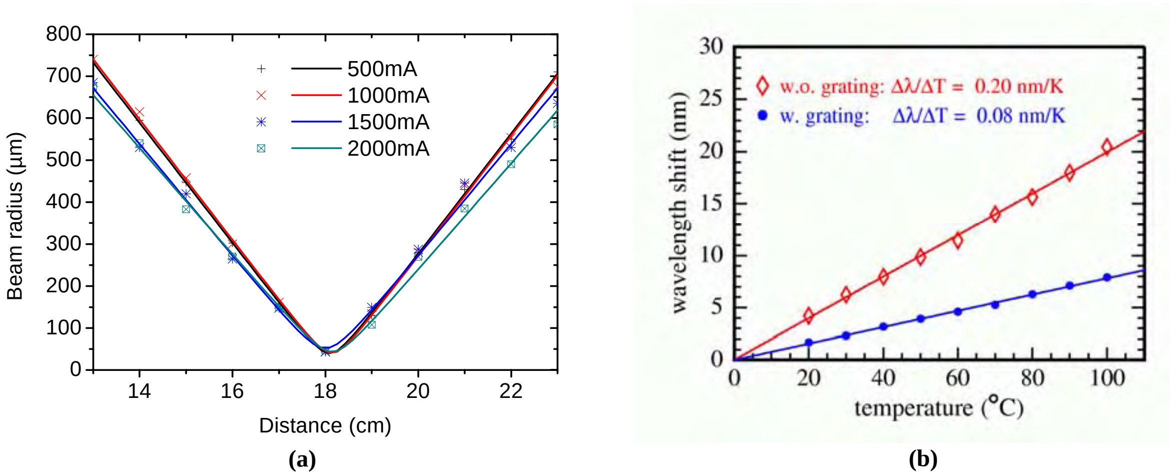

Figure 5: a) Beam radius versus focal distance for different drive currents. b) Plot of the wavelength versus temperature for a tapered laser based on quantum dots with and without frequency selective grating.

7. Coupled cavity devices

The multi-segment laser described here is composed of two coupled cavities with slightly different lengths. Both cavities support a set of Fabry-Perot modes with a spacing inversely proportional to the cavity length. Since the mode spacing of the two cavities is not equal, the two sets of modes coincide only at one particular wavelength within the gain curve of the laser.

The tuning principle of such a device is illustrated in Fig. 6. The mode spacing of the two cavities with different length is λ_1 and λ_2. Tuning is achieved by a variation of the drive current in one or both segments. The temperature change associated with the increased current results in a higher refractive index of this particular segment. This leads to a shift of one set of modes, and the emission switches to the next overlap of modes. Starting from the mode arrangement shown in the central plot of Fig. 6, a shift of the modes in the longer cavity (orange) results in a jumps of the emission by λ_1 (upper plot). A shift of the modes in the shorter cavity results in an opposite tuning of the laser emission by λ_2 (lower plot).

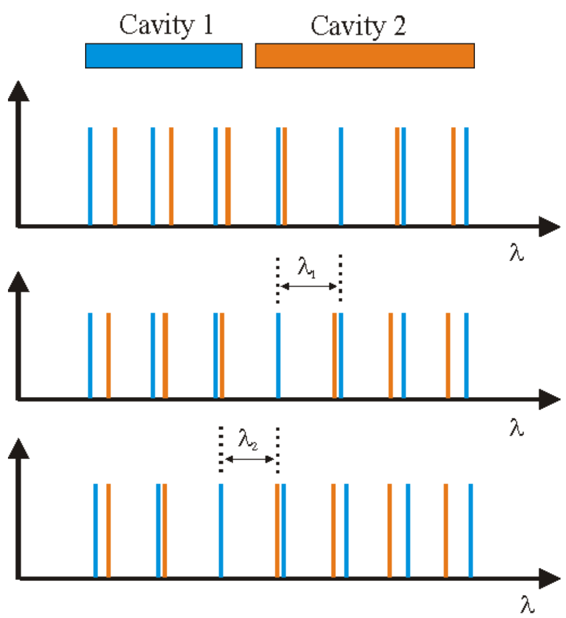

Figure 6: Tuning principle of the coupled cavity laser with a short cavity 1 and a longer cavity 2. A small shift of the modes in one segment causes a large shift of the emission wavelength.

In the design used here, one cavity is formed by a ridge waveguide and the second cavity by a short ridge section and the taper (Fig. 1c). The total length of the device is 800 µm, the two cavities have approximately the same length. In order to achieve a high reflectivity, the width of the trench that separates the two cavities has to be an odd multiple of $\lambda/(4n)$, where n is the refractive index of the planarisation material (BCB).

Fig. 7a shows the emission spectrum of a coupled cavity tapered laser. A SMSR of over 40 dB is obtained. The contour plot in Fig. 7b shows the emission wavelength as a function of the two drive currents. When only one current is changed (horizontal or vertical cut through Fig. 7b), the emission of the devices changes in discrete steps corresponding to the Fabry-Perot mode spacing of one cavity. When the wavelength is tuned sufficiently far away from the centre of the gain curve, another mode coincidence of the two segments becomes more favourable in terms of threshold gain and the emission wavelength jumps by 15-20 nm. The wavelength tunes much faster when the second current is changed due to the much smaller area of the corresponding segment (rear ridge waveguide). The output power of the devices is currently limited to a few hundred mW, limited by the short taper section. Devices with a larger taper are expected to have output power of a few Watts.

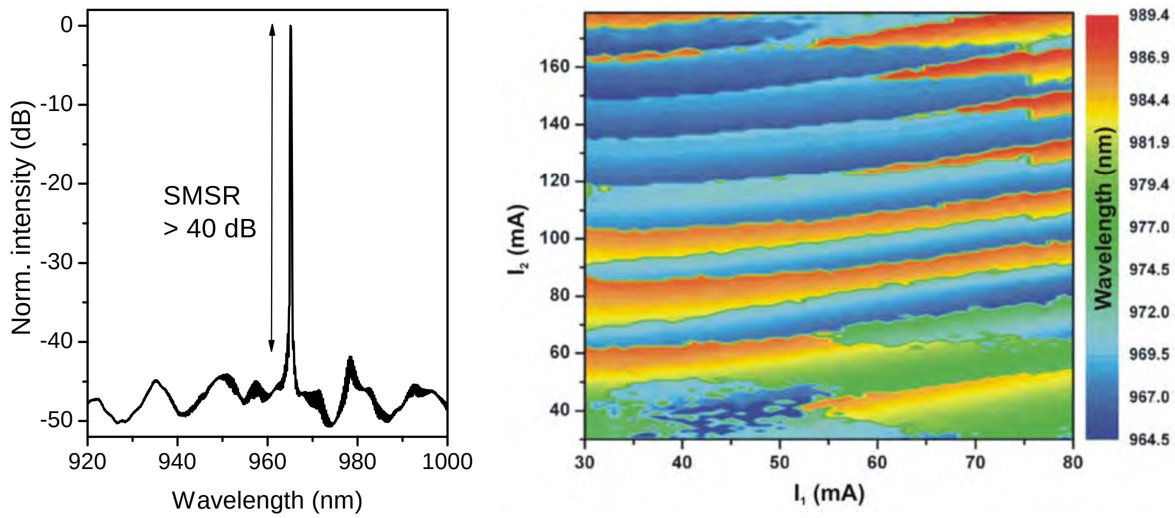

(a) (b)

Figure 7: Emission spectra of a tapered two-segmented device – a) Single mode emission with a SMSR of more than 40dB, b) Tuning characteristic of a coupled cavity laser.

8. Conclusion

A number of approaches for the realisation of single mode tapered lasers with overgrowth free fabrication technology have been discussed. The use of lateral feedback gratings, a concept which is quite successful for ridge waveguides with small output powers, is limited by the small coupling coefficients caused by the large optical waveguides of high power laser layers. A more promising approach seems to be the use of a DBR grating at the rear end of the ridge waveguide sections. Output powers of 1 W, together with stable single mode emission (SMSR ≈ 45 dB) and a good beam quality factor ($M^2 < 2$), have been achieved with these devices. Devices based on two coupled cavities allow a tuning of the emission wavelength over a range of 15-20 nm.

References

[1] J.N. Walpole, "Semiconductor amplifiers with tapered gain regions", *Opt. Quantum Electron.* **28,** 623-645 (1996)

[2] N. Michel, M. Krakowski, I. Hassiaoui, M. Calligaro, M. Lecomte, O. Parillaud, P. Weinmann, C. Zimmermann, W. Kaiser, M. Kamp, A. Forchel, E.-M. Pavelescu, J.-P. Reithmaier, B. Sumpf, G. Erbert, M. Kelemen, R. Ostendorf, J.M. García-Tijero, H. Odriozola and I. Esquivias, "High-brightness quantum well and quantum dot tapered lasers", *Proc. SPIE* **6909,** 690918 (2008)

[3] T.W. Johannes, A. Rast, W. Harth and J. Rieger, "Gain coupled DFB lasers with a titanium surface Bragg grating", *Electron. Lett.* **31,** 370-371 (1995)

[4] M.L. Osowski, J.S. Hughes, R.M. Lammert and J.J. Coleman, "An asymmetric cladding gain-coupled DFB laser with oxide defined metal surface grating by MOCVD", *IEEE Photon. Technol. Lett.* **9,** 1460-1462 (1997)

[5] N. Finger, W. Schrenk and E. Gornik, "Analysis of TM-polarized DFB laser structures with metal surface gratings", *IEEE J. Quantum Electron.* **36,** 780-786 (2000)

[6] K. Mathwig, W. Kaiser, A. Somers, J.P. Reithmaier, A. Forchel, K. Ohira, S.M. Ullah and S. Arai, "DFB Lasers With Deeply Etched Vertical Grating Based on InAs–InP Quantum-Dash Structures", *IEEE Photon. Technol. Lett.* **19,** 264-266 (2007)

[7] W.Y. Choi, J.C. Chen and C.G. Fonstad, "Evaluation of coupling coefficients for laterally-coupled distributed feedback lasers", *Jpn. J. Appl. Phys.* **35,** 4654-4659 (1996)

[8] M. Kamp, J. Hofmann, F. Schäfer, M. Reinhard, M. Fischer, T. Bleuel, J.P. Reithmaier and A. Forchel, "Lateral coupling - a material independent way to complex coupled DFB lasers", *Opt. Mat.* **17,** 19-25 (2001)

[9] R. D. Martin, S. Forouhar, S. Keo, R.J. Lang, R. G. Hunsperger, R.C. Tiberio and P.F. Chapman, "CW performance of an InGaAs-GaAs-AlGaAs laterally-coupled distributed feedback (LC-DFB) ridge laser diode", *IEEE Photon. Technol. Lett.* **7,** 244-246 (1995)

[10] Y. Watanabe, N. Chen, K. Takei, K. Chikuma, N. Futakuchi and Y. Nakano, "Laterally coupled strained MQW ridge waveguide distributed feedback laser diode fabricated by wet-dry hybrid etching process," *IEEE Photon. Tech. Lett.* **10,** 1688-1690 (1998)

[11] M. Kamp, J. Hofmann, A. Forchel, F. Schäfer and J.P. Reithmaier, "Low-threshold high-quantum-efficiency laterally gain-coupled InGaAs/AlGaAs distributed feedback lasers", *Appl. Phys. Lett.* **74,** 483-485 (1999)

[12] M. Kamp, M. Schmitt, J. Hofmann, F. Schäfer, J.P. Reithmaier and A. Forchel, "InGaAs/AlGaAs quantum dot DFB lasers operating up to 213°C", *Electron. Lett.* **35,** 2036-2037 (1999)

[13] M. Reinhardt, M. Fischer, M. Kamp, J. Hofmann and A. Forchel, "1.3-µm GaInNAs-AlGaAs distributed feedback lasers", *IEEE Photon. Technol. Lett.* **12,** 239-241 (2000)

[14] J. Seufert, M. Fischer, M. Legge, J. Koeth, R. Werner, M. Kamp and A. Forchel, "DFB laser diodes in the wavelength range from 760 nm to 2.5 µm", *Spectrochimica Acta Part A* **60,** 3243-3247 (2004)

[15] M. Hümmer, K. Rößner, T. Lehnhardt, M. Müller, A. Forchel, R. Werner, M. Fischer and J. Koeth, "Long wavelength GaInAsSb-AlGaAsSb distributed-feedback lasers emitting at 2.84 µm", *Electron. Lett.* **42,** 583-584 (2006)

[16] R.M. Lammert, J.S. Hughes, S.D. Roh, M.L. Osowski, A.M. Jones and J.J. Coleman, "Low-threshold narrow-linewidth InGaAs–GaAs ridge-waveguide DBR lasers with first-order surface gratings," *IEEE Photon. Technol. Lett.* **9,** 149-151 (1997)

[17] L.A. Coldren, B.I. Miller, K. Iga and J.A. Rentschler, "Monolithic two-section GaInAsP/InP active-optical-resonator devices formed by reactive ion etching", *Appl. Phys. Lett.* **38,** 315-317 (1981)

[18] M. Müller, T. Lehnhardt, A. Bauer, K. Rößner, M. Hümmer and A. Forchel, "Highly integrated widely tunable single mode laser with on-chip power control", *Nanotechnology* **18,** 315203 (2007)

[19] J. Patchell, D. Jones, B. Kelly and J. O'Gorman, "Specifying the wavelength and temperature tuning range of a Fabry-Perot laser containing refractive index perturbations", *Proc. SPIE* **5825,** 1-13 (2005)

[20] W. Kaiser, S. Deubert, J.P. Reithmaier and A. Forchel, "Single-mode tapered quantum dot laser diodes with monolithically integrated feedback gratings", *Electron. Lett.* **43,** 926-927 (2007)

[21] S. Deubert, R. Debusmann, J.P. Reithmaier and A. Forchel, "High-power quantum dot lasers with improved temperature stability of emission wavelength for uncooled pump sources", *Electron. Lett.* **41,** 1125-1127 (2005)

Development and Application of a Spectral Laser Model

J.J. Lim[1], Z. Zhang[1], S. Sujecki[1], S. Bull[1], P.J. Bream[1], A.J. Kent[1],
G. Pauliat[2], N Dubreuil[2], and E.C. Larkins[1]

[1] The University of Nottingham, University Park, Nottingham, NG7 2RD, U.K.
[2] Laboratoire Charles Fabry de l'Institut d'Optique, Campus Politechnique, D128, 91127 Palaiseau, France

1. Introduction

High-power, high-brightness semiconductor laser diodes are currently used in many applications. Often it is not just the power and beam quality of a laser which are important, but also its spectral performance [1]. As an application example, Fig. 1(a) shows the absorption spectrum of a Yb/Er-doped fibre amplifier which has a full width at half maximum (FWHM) of 6 nm at a centre wavelength of ~975 nm. To efficiently pump the fibre amplifier, 975 nm lasers with a narrow emission spectrum ($\Delta\lambda \leq 3$ nm) are required, which remain stable as a function of bias. Unoptimised devices are generally multimode in nature (see Fig. 1(b)) and are not able to satisfy this stringent requirement, hence the necessity for simulation tools which are able to optimise its spectral performance. The analysis of the spectral properties of semiconductor lasers is also important for many other applications of these devices, which include the nonlinear frequency doubling and external cavity lasers using photorefractive crystals.

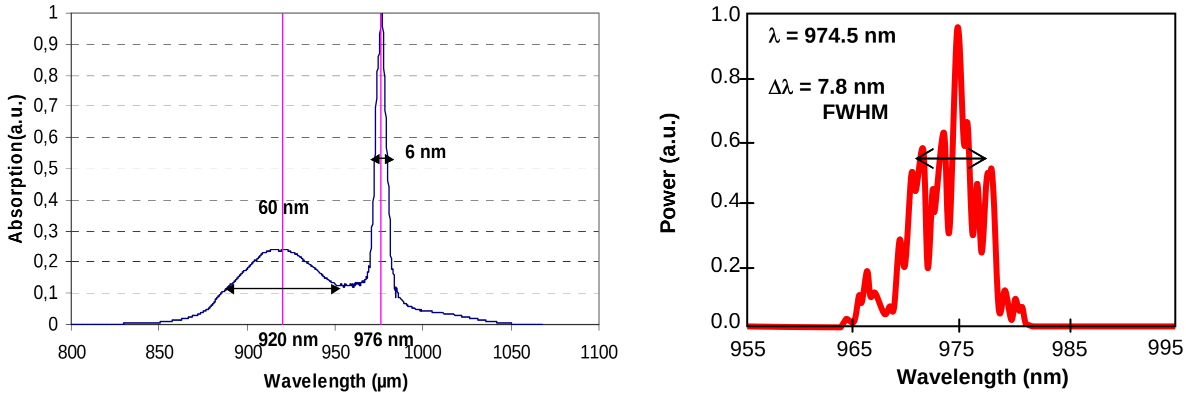

(a) (b)

***Figure 1:** (a) Absorption spectrum of an Yb/Er-doped fibre amplifier (courtesy of Alcatel); (b) Emission spectrum of an early, unoptimised 975 nm tapered laser bar (courtesy of III-V Lab).*

Currently the standard steady state design tools for high power laser diodes are based on quasi-3D single wavelength steady-state models, which neglect amplified spontaneous emission (ASE) and nonequilibrium gain effects [2], [3]. Spectral design tools have only recently been started to be developed. Alongside multi-wavelength optical wave propagation, a spectral laser diode model has to include the scattering and generation/recombination processes responsible for carrier heating (CH) and spectral hole burning (SHB), so that the optical nonlinear interactions between cavity modes can be studied [4]. In this paper, we report on the development and application of a computationally efficient spectral laser model, which is suitable for the simulation and design of high-brightness quantum well (QW) lasers with large cavity geometries. In Section 2, we briefly describe the spectral laser model, Speclase, which considers the optical modes and their coupling through ASE, but does not include nonlinear mode coupling. In Section 3, we describe the dynamic gain model, which is used to obtain the nonequilibrium, steady-state gain and spontaneous emission spectra. The simulation conditions were selected to assess the relative importance of CH and SHB on the spectral properties of the laser (especially with respect to gain compression) and are compared with experimentally measured intracavity spontaneous emission spectra. In Section 4, we apply Speclase to calculate the characteristics of a 1060nm distributed Bragg reflector (DBR) tapered laser. In Section 5, we study the spectral properties of a self-organising external cavity laser using a photorefractive crystal in the external feedback path.

2. Description of spectral model

The 2.5D spectral laser model is based on a single wavelength steady state continuous wave (CW) model, the full details of which have been published elsewhere [3]. This model consists of 2D isothermal optical (x-z) and electrical (x-y) solvers (see Fig. 2). The electrical model is coupled to the optical model through carrier-induced changes in the complex refractive index. The optical model is coupled to the electrical model through stimulated emission/absorption and spontaneous emission coupling. The optical model propagates multiple wavelengths between electrical slices using the 2D Wide-Angle Finite-Difference Beam Propagation Method (WA-FD-BPM) [5], where the effective index assumption [6] has been used. Nonlinear optical coupling of longitudinal modes [7] has been neglected.

The electrical model calculates the carrier density profile for a series of 2D transverse slices along the laser cavity and includes drift-diffusion transport and the capture/escape processes between the bound and unbound states of the QW(s). The photon density distribution at each wavelength is provided as an input to the electrical solver. The gain and spontaneous emission spectra, which are dependent on the photon, electron and hole densities, are obtained from the parameterised dynamic gain model (described in Section 3) and then used by the optical model to propagate the fields to the next electrical slice. The electrical and optical models are solved self-consistently, following an accelerated Fox-Li iterative approach [8].

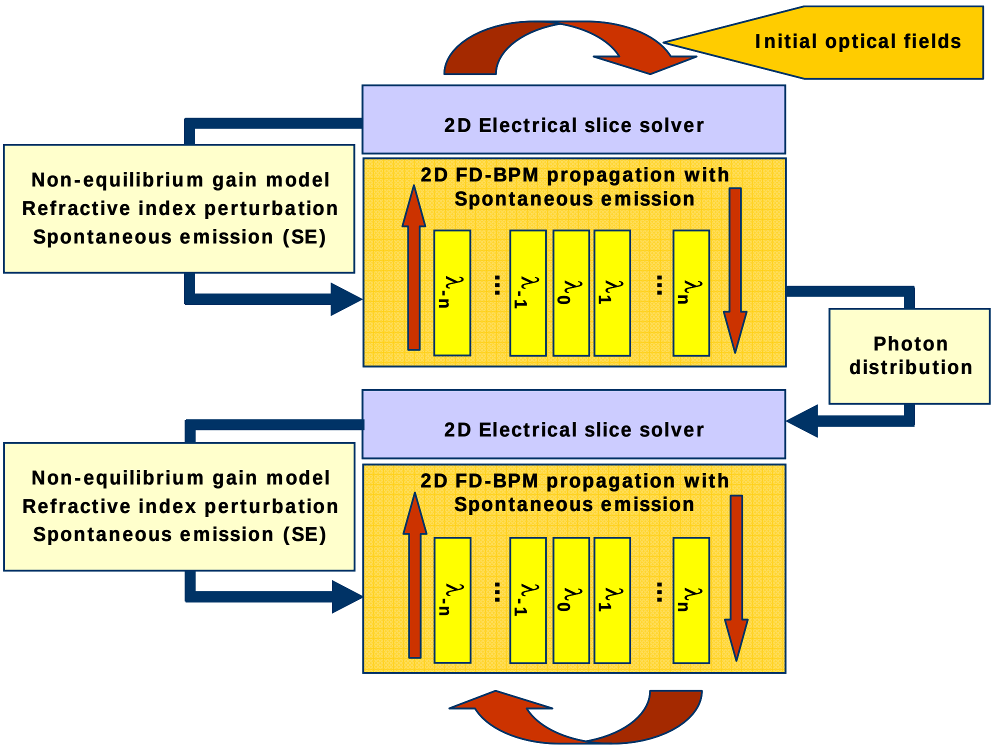

Figure 2: Flow diagram showing the implementation of the spectral laser model [9].

3. Non-equilibrium gain

The dynamic gain model calculates changes in the carrier energy distributions in the QW by intra- and inter-subband relaxation processes, under the influence of electrical and optical excitation. Carrier–carrier scattering, carrier–phonon scattering, carrier capture/escape and radiative/nonradiative recombination processes are included. The gain and spontaneous emission spectra are derived from the band structure, which is obtained from **k.p** calculations and includes the anisotropy of the electronic structure of the strained QWs. Full details of the model can be found in [10]. The dynamic gain model is too computationally intensive to include directly in a spatially resolved laser simulator. Consequently, the gain and spontaneous emission spectra from the dynamic gain model are parameterised as a function of QW carrier density, intracavity photon density and wavelength.

The parameterisation of the gain and spontaneous emission is performed as follows: Firstly, the dynamic gain model is used to calculate the nonequilibrium steady-state gain and spontaneous emission spectra for the range of CW electrical and optical excitation conditions required by the spectral laser model. Fermi–Dirac distributions are fit to the calculated carrier distributions, conserving the total carrier density and total carrier energy in each subband. The resulting gain and spontaneous emission spectra, $g(E_{ph})$ and $R_{sp}(E_{ph})$, are the quasi-equilibrium spectra, which include only CH. Finally, the standard phenomenological gain compression is introduced using Eq. (1) to account for SHB, where S_{tot} is the total photon density and ε is the gain compression coefficient.

$$g_{SHB}(E_{ph}) = \frac{g(E_{ph})}{1+\varepsilon S_{tot}} \tag{1}$$

The spectral laser model was used to simulate a ~975nm 2mm long tapered (<1°) laser based on a 9nm InGaAs/InGaAsP single QW. The ridge waveguide and tapered amplifier lengths were 500 and 1500μm, respectively. These calculations were performed at three different biases (1.41, 1.47 and 1.53 V), using both equilibrium and nonequilibrium gain, with a gain compression factor, $\varepsilon = 7\times10^{-23}$ m^3.

Fig. 3(a) shows the simulated equilibrium and nonequilibrium spontaneous emission spectra at the centre of the front facet. The increase in the spontaneous emission near the lasing wavelength is expected because of the increase in carrier density required to compensate the gain compression and is an indication of SHB. The magnitude of the spontaneous emission rate near the lasing wavelengths for each bias is similar for both sets of simulations, as expected. Fig. 3(b) shows a close-up of the CB1–LH1 (1st light hole) transition around 908 nm. Increasing bias leads to a stronger CB1-LH1 transition. This is caused by carrier heating, which results in more carriers in the higher subbands.

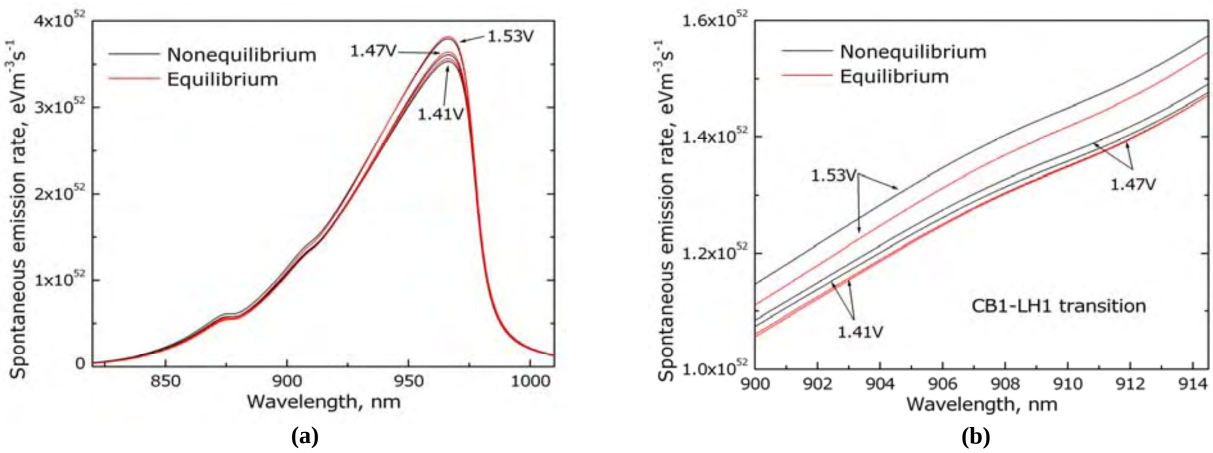

Figure 3: (a) Calculated equilibrium and nonequilibrium spontaneous emission spectra with varying bias taken at the centre of the front facet; (b) close-up of the CB1–LH1 transition [9].

Finally, Fig. 4 shows intracavity spontaneous emission spectra from micro-electroluminescence measurements [11] at various bias currents. The uncalibrated spectra have been corrected for the spectral response of the Ge detector and were measured through the windowed contacts of a 4◦ tapered laser diode with the same epitaxy as the simulated device. The spikes in the measurements above threshold are caused by scattered stimulated emission. These results are in good qualitative agreement with those in Fig. 3. The carrier density continues to increase above threshold because of SHB, and the CB1-LH1 transition increases more quickly because of CH.

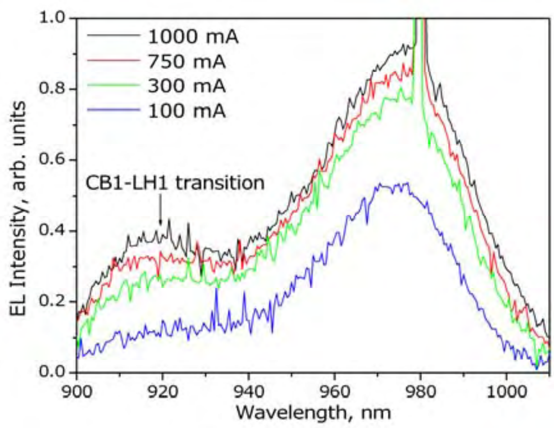

Figure 4: Experimentally measured intracavity spontaneous emission spectra with varying bias [9].

4. 1060nm tapered DBR laser

In this section, we use the example of a high-power tapered DBR laser (Fig. 5) to demonstrate the advantages of the spectral simulation tool. The tapered DBR laser is divided into three longitudinal sections: the DBR section (1 mm), the RW section (1 mm) and the tapered section (2 mm). The tapered section has a full angle of 4° and the output aperture is approximately 144 μm wide. Since the DBR section is passive (unpumped), we have for the moment represented it by a fixed reflectivity.

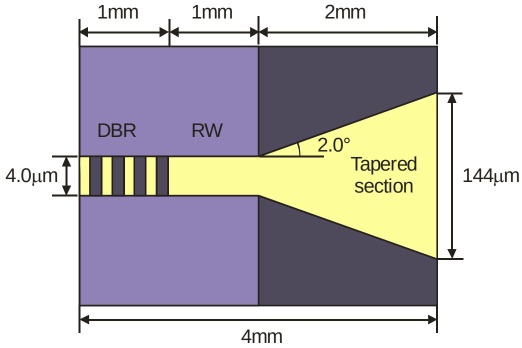

Figure 5: Geometrical structure of the 1060 nm DBR tapered laser.

A spectral simulation of the tapered laser was performed with a common contact bias of 1.4 V. The reflectivity spectrum of the DBR was calculated based on an analytical formula derived from coupled mode theory:

$$|r|^2 = \frac{\kappa^2}{\delta^2 + (\kappa^2 - \delta^2)\coth^2(L\sqrt{\kappa^2 - \delta^2})} \tag{2}$$

where κ = 18 cm^{-1}, L = 1 mm and δ is the phase deviation which is related to the wavelength change Δλ by:

$$\delta = -\frac{2\pi c\lambda^2}{v_g \Delta\lambda} \tag{3}$$

The calculated reflectivity spectrum is shown in Fig. 6(a) with a peak reflectivity at 1053.75 nm. In the spectral simulation, we have only used 21 wavelength points due to memory and computational constraints. We have performed spectral simulations both with and without the DBR and the resulting output power spectra are shown in Fig. 6(b) after 100 roundtrips. (For the case without DBR, the back facet reflectivity is assumed to be fixed at 90%.) It is seen that the DBR at the back facet has significantly narrowed the output power spectra and locked the lasing wavelength to the peak reflectivity position. Without the DBR, the output spectrum is broader and centred at a wavelength of 1054 nm. The spectrum without the DBR has not converged to a single mode after 100 roundtrips. This is because the wavelength spacing is small, so that all modes experience quite similar optical gain. It is, however, noted that the total power of all of the modes is the same with or without the DBR (without gain compression) and has converged to a value of 660 mW.

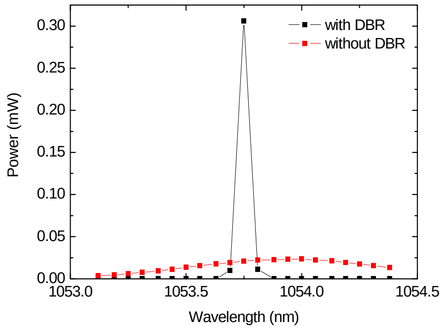

(a)

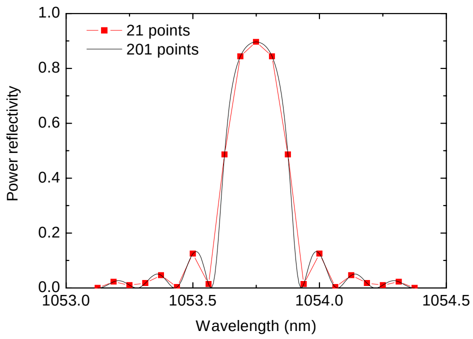

(b)

Figure 6: (a) Power reflectivity spectrum of Bragg grating; (b) output power spectrum of tapered laser with and without DBR at V_{taper}=V_{ridge}=1.4 V.

5. Self-organising external cavity lasers

Another application considered here comprises of a high power laser operating in an external cavity with a self adapting spectral filter [12] provided by a photorefractive crystal (see Fig. 7). The model of this external cavity laser consists of a spectral model of the semiconductor tapered amplifier described in Section 3 and a plane wave model of the photorefractive crystal, which provides wavelength selective feedback [12]. The laser operates at a nominal wavelength of about 975 nm. The parameters of the simulated structure of the tapered laser are summarised in Table 1.

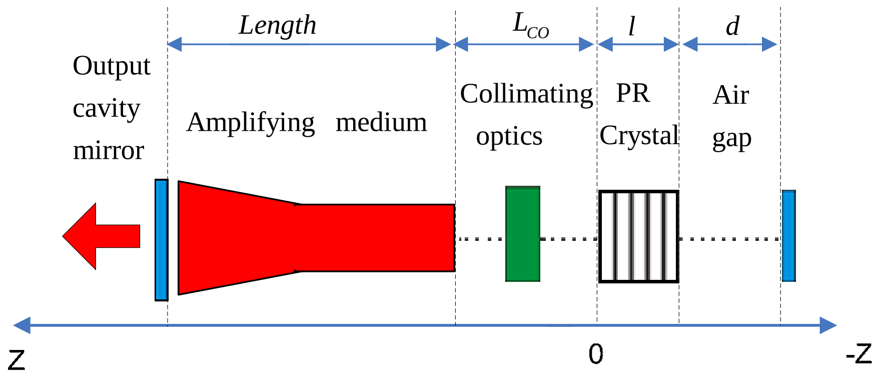

Figure 7: General scheme for a self-organising cavity tapered laser cavity based on an adaptive Fabry-Perot filter.

Name	Value	Unit	Description
W	50	μm	Output facet width
Length	2500	μm	Total length of tapered laser
R_o	0.01		Output facet reflectivity
β_{sp}	1.0×10^{-20}		Spontaneous emission coupling factor
W_{feed}	3.5	μm	Ridge waveguide width
L_{feed}	500	μm	Ridge waveguide length
Angle	0.32	degree	Taper angle
dn/dN	4.1×10^{-14}	$m^{3/2}$	n : refractive index; N : carrier density
n_g	3.9		Group refractive index
n_{tl}	3.5		Refractive index
l	0.3	cm	Length of photorefractive crystal
d	3.0	cm	Air gap length
Γ	5.0	cm^{-1}	Photorefractive gain coefficient
n	2.4		Refractive index
R_m	0.90		Reflectivity of right mirror

Table 1: Parameters of the self organising external cavity laser.

Figure 8 shows the calculated output spectrum at the bias current of 0.55 A and the light current characteristics. These results confirm that the inclusion of the photorefractive crystal in the external feedback loop forces the laser cavity into single mode operation. From experimental results, it is known that without the photorefractive crystal the laser emits light in a number of longitudinal modes with a typical spectral emission width of 1 nm.

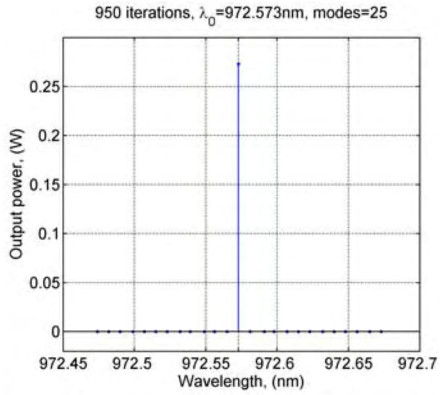

(a)

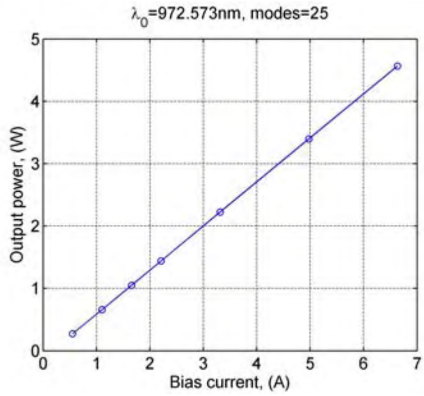

(b)

Figure 8: Output spectrum (a) and light-current characteristics (b) of the laser.

6. Summary

We have extended our monochromatic 2.5D laser model to simulate spectral effects by including the optical fields at different wavelengths and spontaneous emission coupling. Such a spectral laser model is important for simulating devices which require a stable and narrow output spectrum. We have demonstrated the application of this model to three specific problems. In the first example, the model was used with a dynamic gain model to investigate gain compression in a tapered laser under different bias conditions. The results show that carrier heating leads to a stronger excited state transition in the spontaneous emission spectra. This observation was confirmed by experimentally measured intracavity spontaneous emission spectra. In the second example, a tapered DBR laser was simulated. It is shown that the inclusion of the DBR at the back facet causes a narrowing of the output power spectra and locks the lasing wavelength to the peak reflectivity position. In the final example, an external cavity laser with a self-adapting photorefractive crystal was simulated. The reflectivity of the photorefractive crystal is modelled by a plane wave model. These simulations show that the photorefractive crystal is effective in suppressing the side modes and forcing the laser to operate in a single longitudinal mode.

7. References

[1] I. Kaminow and T. Li (eds.), Optical Fiber Telecommunications, Academic Press, San Diego, 2002.

[2] S. Sujecki, L. Borruel, J.G. Wykes *et al.*, "Quasi-3-D simulation of high-brightness tapered lasers," IEEE J. Select. Topics Quantum Electron., Vol. 9, p. 823, 2003.

[3] J.J. Lim, T.M. Benson and E.C. Larkins, "Design of wide-emitter single-mode laser diodes," IEEE J. Quantum Electron., Vol. 41, p. 506, 2005.

[4] B.E.A. Saleh and M.C. Teich, Fundamentals of Photonics, John Wiley & Sons, Inc., Toronto, 1991.

[5] G.R. Hadley, "Multistep method for wide-angle beam propagation," Opt. Lett., Vol. 17, p. 1743, 1992.

[6] H.C. Casey Jr. and M.B. Panish, Heterostructure Lasers Part A: Fundamental Principles, Academic Press, Inc., London, 1978.

[7] R.F. Kazarinov, C.H. Henry and R.A. Logan, "Longitudinal mode self-stabilization in semiconductor-lasers," J. Appl. Phys., Vol. 53, p. 4631, 1982.

[8] G.P. Agrawal, "Fast-Fourier-Transform based beam-propagation model for stripe-geometry semiconductor-lasers – inclusion of axial effects," J. Appl. Phys., Vol. 56, p. 3100, 1984.

[9] P.J. Bream, J.J. Lim, S. Bull *et al.*, "The impact of nonequilibrium gain in a spectral laser diode model," Optical and Quantum Electronics, Vol. 38, p. 1019, 2006.

[10] P.J. Bream, S. Sujecki and E.C. Larkins, "Investigation of nonequilibrium steady state gain in semiconductor quantum wells," IEE Proc. Optoelectron., Vol. 153, p. 299, 2006.

[11] S. Bull, A.V. Andrianov, J.G. Wykes *et al.*, "Quantitative imaging of intracavity spontaneous emission distributions using tapered lasers with windowed n-contacts," IEE Proc. Optoelectron., Vol. 153, p. 2, 2005.

[12] G. Pauliat, N. Dubreuil and G. Roosen, Photorefractive Materials and Their Applications 3: Applications, Springer Series in Optical Science 2007, pp. 253-275.

TOXICOLOGY AND SAFETY WORKSHOP

Nicole Proust, a clean technology expert from Thales Research and Technology, France, recently organised a workshop supported by the WWW.BRIGHTER.EU project on "Toxicology and Safety". The workshop took place at Thales Research and Technology (TRT) in Palaiseau, France on Wednesday 13th February 2008.

The half-day Workshop, attended by around 40 delegates from across Europe, included a program of 5 presentations – 3 given by invited speakers from outside the Consortium and 2 given by members of the BRIGHTER project team.

The program (see below) began with a short 15 minute video introduction to the BRIGHTER project, its objectives and targeted applications.

The entire workshop was video recorded and the presentations will be released in RichMedia CD format in the near future. The presentations from the workshop and the project video clip will be available soon on the project website, which can be found at: http://www.ist-brighter.eu.

THALES

Toxicology and Safety Workshop

Thales Research and Technology, Palaiseau, France
Wednesday 13th February 2008, 08:30 – 12:30

Programme

BRIGHTER : An introduction
A 15 minute video overview of the project, its objectives and targeted applications

Toxicology : A basic introduction.
Dr. J.H. Duffus – Director, Edinburgh Centre for Toxicology, Scotland

Respiratory exposure to gases and particles
Dr. C. Lesne – Medical Doctor, Rennes 1 University France

Toxicology : Examples related to As, Al, Be, Ga and In compounds
N. Proust – Clean Technology Expert, Thales TRT, France, BRIGHTER Partner

MBE maintenance : Safety management.
Prof. J.P. Reithmaier – Professor, University of Kassel, Germany, BRIGHTER Partner

Nanotoxicology : The nanoparticles example
Dr. A. Lombard – Toxicologist, Alotoxconsulting, France

RICH MEDIA CDs

What are RichMedia CDs?

RichMedia CDs are an innovative way of distributing presentations (e.g. from tutorials and / or workshops) that allows the inclusion of the speakers comments together with the presentation slides. This novel format has a clear enhanced value for presentations that are used as teaching materials (compared to the presentation slides alone). The content can be distributed not only CDs, but also online.

In a RichMedia presentation, the screen is divided in to 3 parts (see example below):

1. Presentation slides
2. Video of the presenter
3. Content and navigation panel

The video, audio and slide changes are all synchronised and a PDF file of the presentation can also be opened from the main window. A screenshot of a RichMedia presentation of a BRIGHTER tutorial is shown below.

RichMedia CDs and BRIGHTER

Over the course of the BRIGHTER project, the Consortium are developing a series of 16 technical training tutorials (see edition 2 of our e-Newsletter for more details), each of which will be produced in the RichMedia CD format. The first of these have been produced and will be available shortly for download from our project website. Others will then appear regularly during the remainder of the project and will be publicised in future e-Newsletters. The presentations from our recent "Toxicology and Safety" workshop will also be available for download alongside the technical tutorials. For further information about BRIGHTER's RichMedia CDs and the RichMedia format in general, please contact Jean Christophe Mielnik at Thales Research and Technology, France (jean-christophe.mielnik@thalesgroup.com).

SELECTED PUBLICATIONS & PRESENTATIONS

Improvements in Diode Laser Performance

- N. Michel, M. Lecomte, O. Parillaud, M. Calligaro, J. Nagle and M. Krakowski, "Optimization of the wall-plug efficiency of Al-free active region diode lasers at 975 nm," SPIE Proceedings Vol. 6997, 69971W, May 2008.
- B. Sumpf, M. Zorn, J. Fricke, P. Ressel, H. Wenzel, G. Erbert, M. Weyers and G. Tränkle, "1 W reliable operation of broad area lasers and 8 W reliable operation of 5 mm wide laser bars at 650 nm," SPIE Proceedings Vol. 6876, 68760T, Feb. 2008.
- B. Sumpf, P. Adamiec, M. Zorn, P. Froese, J. Fricke, P. Ressel, H. Wenzel, M. Weyers, G. Erbert and G. Tränkle, "650 nm tapered lasers with 1 W maximum output power and nearly diffraction limited beam quality at 500 mW," SPIE Proceedings Vol. 6876, 68760M, Feb. 2008.
- R. Ostendorf, G. Kaufel, R. Moritz, M. Mikulla, O. Ambacher, M.T. Kelemen and J. Gilly, "10 W high-efficiency high-brightness tapered diode lasers at 976 nm," SPIE Proceedings Vol. 6876, 68760H, Feb. 2008.
- N. Michel, M. Lecomte, O. Parillaud, M. Krakowski, J.M. García-Tijero and I. Esquivias, "Asymmetric Al-free active region laser structure for high-brightness tapered lasers at 975 nm," SPIE Proceedings Vol. 6909, 69090R, Feb. 2008.
- N. Michel, M. Krakowski, I. Hassiaoui, M.Calligaro, M. Lecomte, O. Parillaud, P. Weinmann, C. Zimmermann, W. Kaiser, M. Kamp, A. Forchel, E.M. Pavelescu, J.P. Reithmaier, B. Sumpf, G. Erbert, M. Kelemen, R. Ostendorf, J.M. García-Tijero, H. Odriozola and I. Esquivias, "High brightness quantum well and quantum dot tapered lasers," SPIE Proceedings Vol. 6909, 690918, Jan. 2008.

Lasers Modules and Diode Laser Applications

- G. Kochem, M. Haverkamp and K. Boucke, "Frequency stabilized high brightness tapered amplifier and laser modules," SPIE Proceedings Vol. 6997, 69971A, May 2008.
- M. Haverkamp, G. Kochem and K. Boucke, "Single mode fiber coupled tapered laser module with frequency stabilized spectrum," SPIE Proceedings Vol. 6876, 68761D, Feb. 2008.
- C.H. Kwok, R.V. Penty, I.H. White, K.-H. Hasler, B. Sumpf and G. Erbert, "Direct modulation of a twin-contact high brightness tapered laser for free space communications applications," Semiconductor and Integrated Opto-Electronics Conference (SIOE 2008), 31st March – 2nd April 2008, Cardiff, Wales, U.K.
- C.H. Kwok, R.V. Penty, I.H. White, K.-H. Hasler, B. Sumpf and G. Erbert, "Twin-contact high brightness tapered laser for high modulation efficiency high speed signal modulation" Submitted to 8th Asia-Pacific Optical Communications Conference (APOC 08), to be held 26th – 30th October 2008, Hangzhou, China.
- D. Gorpas, K. Politopoulos and D. Yova, "A binocular machine vision system for three-dimensional surface measurement of small objects," Computerised Medical Imaging and Graphics, Vol. 31, pp. 625-637, Dec. 2007.

External Cavity Lasers & Frequency Doubling

- J. Lundeman, O. Jensen, P. Andersen, S. Andersson-Engels, B. Sumpf, G. Erbert and P.M. Petersen, "High power 404 nm source based on second harmonic generation in PPKTP of a tapered external feedback diode laser," Optics Express, Vol. 16, pp. 2486-2493, 2008.
- I. Hassiaoui, N. Michel, G. Bourdet, R. McBride, M. Lecomte, O. Parillaud, M. Calligaro, M. Krakowski and J.P. Huignard, "Very compact external cavity diffraction-coupled tapered laser diodes," Applied Optics, Vol. 47, pp. 746-750, 2008.
- I. Hassiaoui, N. Michel, M. Lecomte, O. Parillaud, M. Calligaro, M. Krakowski, G. Bourdet and J.P. Huignard, "Diffraction coupling of tapered lasers in a very compact external Talbot cavity," SPIE Proceedings Vol. 6997, 699705, May 2008.
- D. Paboeuf, G. Lucas-Leclin, P. Georges, B. Sumpf, G. Erbert, C. Varona, P. Loiseau, G. Aka and B. Ferrand, "Diode pumping of Nd:ASL and its frequency doubling for blue emission around 450 nm," SPIE Proceedings Vol. 6871, 68711P, Mar. 2008.

Diode Laser Physics, Degradation & Reliability

- M. Ziegler, J.W. Tomm, T. Elsaesser, G. Erbert, F. Bugge, W. Nakwaski and R.P. Sarzała, "Visualization of heat flows in high-power diode lasers by lock-in thermography," Applied Physics Letters, Vol. 92, 103513, 2008.
- M. Ziegler, J.W. Tomm, T. Elsaesser, C. Matthiesen, M. Bou Sanayeh and P. Brick; "Real-time thermal imaging of catastrophic optical damage in red-emitting high-power diode lasers," Applied Physics Letters, Vol. 92, 103514, 2008.
- M. Ziegler, J.W. Tomm, F. Weik, T. Elsaesser, C. Monte, J. Hollandt, H. Kissel, G. Seibold and J. Biesenbach, "Accurate determination of absolute temperatures of GaAs based high-power diode lasers," SPIE Proceedings Vol. 6876, 68761A, Feb. 2008.
- S. Bull, J.W. Tomm and E.C. Larkins, "Identification of degradation mechanisms in high-power laser bars using by-emitter degradation studies," Journal of Materials Science: Materials in Electronics, published online DOI 10.1007/s10854-008-9577-5, Jan. 2008.
- A. Martín-Martín, M. Avella, M. Pommiès, J. Jiménez, M. P. Iñiguez, M. Oudart and J. Nagle, "Study of the degradation of AlGaAs-based high-power laser bars: V defects," Journal of Materials Science: Materials in Electronics, published online DOI 10.1007/s10854-007-9512-1, Dec. 2007.
- M. Maziarz, B. Piechal, A. Bercha, R. Bohdan, W. Trzeciakowski and J.A. Majewski, "Pressure and temperature dependence of threshold current in semiconductor lasers based on InGaAs/GaAs quantum-well systems," Acta Physica Polonica A, Vol. 112, pp. 437-442, 2007.

Laser Diode Design, Modelling & Optimisation

- L. Borruel, H. Odriozola, J.M.G. Tijero, I. Esquivias, S. Sujecki and E. C. Larkins, "Design strategies to increase the brightness of gain-guided tapered pasers," Optical and Quantum Electronics, published online DOI 10.1007/s11082-008-9187-8, Feb. 2008.
- J.M.G. Tijero, H. Odriozola, L. Borruel, I. Esquivias, S. Sujecki and E. C. Larkins, "Enhanced brightness of tapered laser diodes based on an asymmetric epitaxial design," IEEE Photonics Technology Letters, Vol. 19, pp. 1640-1642, 2007.

PROJECT e-NEWSLETTERS

Don't miss the next WWW.BRIGHTER.EU e-Newsletter!

Look out for the following in Edition 4 in October 2008:

- Partner profiles – *Ferdinand Braun Institute, LCFIO, Risø, University of Madrid*
- "Behaviour and performance of external cavity lasers" – *University of Nottingham, Risø, LCFIO, Thales Research and Technology*
- "Interstitial photodynamic therapy" – *Biolitec*
- "Mirror heating in high power lasers" – *University of Madrid, Max Born Institute*
- "High-Brightness lasers with multi-contacts" – *Ferdinand Braun Institute*


e-Newsletter n°4
October 2008
WWW.BRIGHTER.EU
World Wide Welfare: High-Brightness Semiconductor Lasers for Generic Use
CONTENT
PROJECT NEWS

e-Newsletter Back Issues

If you missed either of our first 2 e-Newsletters, or would like to see our 3 e-Newsletters from the earlier WWW.BRIGHT.EU project, please visit out website at http://www.ist-brighter.eu, where PDF copies of all published e-Newsletters can be downloaded.

Some highlights of previous e-Newsletters!

Applications Articles

- Optical wireless communication systems
- High-power laser diode collimators
- Frequency-doubled laser diodes
- Pumping of fibre lasers

……and many more

Technical Papers

- By-emitter degradation analysis of high-power laser bars
- Next generation high-power quantum dot laser materials
- Pressure and temperature tuning of laser diodes
- Design of high-power high-brightness lasers

……and many more


Technology and Applications of Frequency-Doubled High-Brightness Laser Diodes

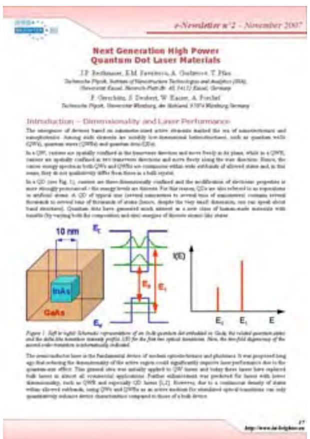
Next Generation High Power Quantum Dot Laser Materials


Pumping of Fibre Lasers

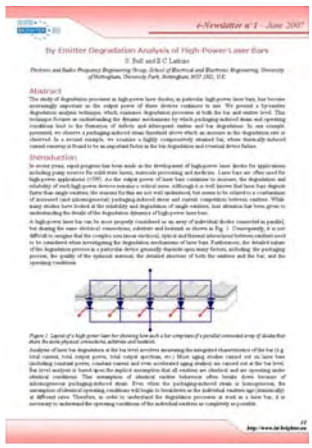

CALENDAR OF EVENTS

The calendar below lists some important events later in 2008 at which the Consortium will be represented.

1st – 5th September
Numerical Simulation of Optoelectronic Devices Conference (NUSOD), *Nottingham, U.K*

14th – 18th September
IEEE International Semiconductor Laser Conference (ISLC), *Sorrento, Italy*

19th – 20th September
European Semiconductor Laser Workshop (ESLW), *Eindhoven, Netherlands*

21st – 25th September
European Conference on Optical Communication (ECOC), *Brussels, Belgium*

26th – 30th October
Asia-Pacific Optical Communications Conference (APOC), *Hangzhou, China*

9th – 13th November
IEEE Lasers & Electro-Optics Society Annual Meeting (LEOS), *Newport Beach, CA, USA*

8th International Conference on
Numerical Simulation of Optoelectronic Devices
1st – 5th September 2008
University of Nottingham, U.K.

Conference Chairs: Joachim Piprek, NUSOD Institute and Eric Larkins, University of Nottingham

The University of Nottingham, the NUSOD Institute and the WWW.BRIGHTER.EU Consortium are pleased to announce that the next international Numerical Simulation of Optoelectronic Devices (NUSOD) conference will be held at the University of Nottingham, U.K, from 31st August to 5th September 2008.

Invited Talks

"Slow and stopped light in metamaterials"
Ortwin Hess, University of Surrey, U.K.

"TiberCAD: Towards multiscale simulation of optoelectronic devices"
Matthias Auf der Maur, University of Rome, Italy

"Nonequilibrium Green's function simulation of quantum cascade lasers"
Tim Schmielau, Sheffield Hallam University, U.K.

"Dynamic simulation of high brightness semiconductor lasers"
Mark Lichtner, Weierstrass Institute, Germany

"Light transformations in metallo-dielectric nanolayers"
Rafal Kotynski, University of Warsaw, Poland

"Accurate modelling of quantum well infrared photodetectors by FDTD"
Gaetano Bellanca, University of Ferrara, Italy

"Perspective on device modelling and simulation in an optoelectronics fab"
Stephen Jones, Bookham, U.K.

Find out more at http://www.nusod.org/conf08
Post deadline papers to be received by 31st July 2008
Online conference registration is now available
Early registration deadline 31st July 2008